

# A review on recent advances in hybrid supercapacitors: Design, fabrication and applications

Aqib Muzaffar<sup>a</sup>, M. Basheer Ahamed<sup>a,\*</sup>, Kalim Deshmukh<sup>a</sup>, Jagannathan Thirumalai<sup>b</sup>

<sup>a</sup> Department of Physics, B.S. Abdur Rahman Crescent Institute of Science and Technology, Chennai 600048, Tamil Nadu, India

<sup>b</sup> Department of Physics, Srinivasa Ramanujan Centre, SASTRA University, Kumbakonam 612001, Tamil Nadu, India

## ARTICLE INFO

### Keywords:

Hybrid supercapacitors

Pseudocapacitors

Electric double layer capacitor

## ABSTRACT

Hybrid supercapacitors with their improved performance in energy density without altering their power density have been in trend since recent years. The hybrid supercapacitor delivers higher specific capacitance in comparison to the existing electric double layer capacitor (EDLC) and pseudocapacitors. Generally, the asymmetric behavior of hybrid supercapacitors which is the combination of EDLC and pseudocapacitor acts as an enhancer in its respective capacitance values. This asymmetric approach marks a new beginning towards the much-needed pollution free, long lasting and proficient energy-storing performance. Corresponding to their utilization in hybrid electric vehicles and similar sort of power necessity based devices; the research in developing new advanced storage devices finds an enormous and vast future ahead. The most significant factor for the energy efficient applications demands a considerably higher ratio of surface to the volume by incorporation of new materials. This review article gives an overview of recent advances in the development of hybrid supercapacitors, storage mechanism, criteria of formation, components, different electrode and electrolyte materials, electrochemical profile assessment, design fabrication and their applications.

## 1. Introduction

The need for efficient energy storage and clean energy alternatives is the one of the prime concern in the modern world. The need can be fulfilled by the application of energy storage devices like supercapacitors, batteries, fuel cells and other energy storing devices. Supercapacitors are the devices devoted to energy storage [1]. They tender sufficient energy and power densities that are intended towards intermediate to inflated power entailing purposes. They are actually storage devices lying between the range of usual capacitors and the batteries [2]. In order to assuage the serious concerns regarding energy crisis, numerous alternative technologies have come into existence [3]. The main aim of the technologies is to reduce greenhouse gas pollution resulting from the expenditure of fossil fuels [4]. One such alternative can be supercapacitors offering elevated power densities, elongated cycle life, quick charge and discharge time intervals as well as being clean and safe means of electrochemical energy storage [5]. Supercapacitors energy storage is based on the accumulation of charge or reversible redox reactions and as such supercapacitors are classified into three main categories depending upon the storage criteria viz; EDLC and pseudocapacitor and their combination being called as the hybrid supercapacitor.

The unconventional energy storing devices like batteries, fuel cells and supercapacitors are based on electrochemical conversions. The advantages of supercapacitor over batteries and fuel cells are long charging/discharging cycles and wide operating temperature range [6]. Hybrid supercapacitors are the devices with elevated capacitance and elevated energy storage capability. They have fetched much limelight due to their tendency of combining the properties of their components (EDLC and pseudocapacitor) [7]. The possibilities for such combinations are numerous with keen interest for the ones formed by conducting and electroactive components proceeding towards the goal of energy storage [8].

The hybrid supercapacitor, which is the combination of EDLC and pseudocapacitor, has more enhanced characteristics than the combining components. In EDLC, the energy storage is based on intrinsic shell area and atomic charge partition length [9]. Whereas as the storage of energy is attained due to rapid repeatable redox reactions among electro-active units lying on active electrode material and an electrolyte solution in pseudocapacitor [10]. The combination of these two storage mechanisms together constitutes the energy storage mechanism of hybrid supercapacitors. One-half of the hybrid supercapacitor acts as EDLC while other half behaves as pseudocapacitor. Comparatively hybrid supercapacitors possess higher energy densities

\* Corresponding author.

E-mail address: [basheerahamed@bsauniv.ac.in](mailto:basheerahamed@bsauniv.ac.in) (M.B. Ahamed).

<https://doi.org/10.1016/j.rser.2018.10.026>

Received 25 July 2018; Received in revised form 1 October 2018; Accepted 30 October 2018

1364-0321/ © 2018 Elsevier Ltd. All rights reserved.

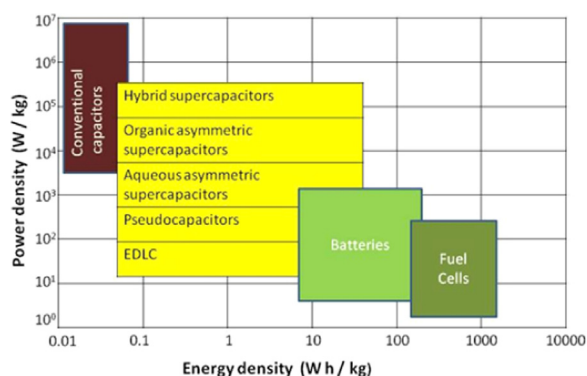


Fig. 1. Ragone Plot for different energy storage devices. Reproduced with permission from Ref. [1] Copyright © 2013 John Wiley and Sons.

as well as power densities than the normal EDLC and pseudocapacitor. This favors towards their use compared to other energy storing devices in energy efficient systems [11]. On the other hand in comparison with fuel cells and batteries; hybrid supercapacitors hit the apex coming to the power density feature but have considerably lower power density compared to conventional capacitor displayed in Ragone plot for different energy storage devices as shown in Fig. 1.

The differentiating aspect of the supercapacitor to the conventional capacitor is the absence of dielectric material [12]. The conventional capacitor consists of dielectric plates for electrostatic charge storage. Whereas supercapacitor (hybrid) comprises of submerged electrodes within electrolyte solution kept apart through a separator prospering electrolytic ions diffusion but hinders the direct contact of electrodes or short circuit [13]. Hybrid supercapacitors may be asymmetric or symmetric based on either two different electrodes, same electrodes with different mass loadings or a combination of two electrodes with the difference in charge storage behavior [14].

In comparison to present rechargeable batteries, the supercapacitors including EDLC, pseudocapacitor and hybrid supercapacitor furnishes much greater power density owing to a characteristic of reactions experienced on the electrode's outer layer for charge storage without endowing to the dispersion of ions into the active species [15]. The present rechargeable batteries are mainly depending on intercalation and de-intercalation of cations controlled by diffusion that restricts their charging and discharging rate or power density [16]. The hybrid supercapacitors possess the ability to store a huge quantity of charge furnished at elevated power rates in comparison to rechargeable batteries [17]. Hence, hybrid supercapacitors promise to be a reciprocal choice compared to rechargeable batteries urging to high power delivery or fast energy yield [18]. However, the charge stored on the surface restricts their energy density or capacity to a lower value in contrast to batteries. In hybrid supercapacitor, energy density prevails because of active materials specific capacitance and net cell voltage [19].

The driving force towards the development of hybrid supercapacitor is concerned with the apprehension of achieving elevated energy density, rapid kinetics, extensive cycle life, enhanced security and subordinate preparatory expenditure [20]. The hybrid supercapacitor systems comprising of non-aqueous redox materials have been the trend in recent times and are enthusiastically investigated and developed [21–25]. In hybrid supercapacitors, the main provoking feature intends towards the development of materials showing superior energy density in near approximation to batteries without altering their ingrained characteristic of high power density along with long cycling life [26].

One of the predominantly efficient methods to achieve that is the development of highly porous and nano-sized electrode material to enhance the capacitance [27]. On the other hand, the development of hybrid supercapacitor efficiently utilizing the potential gap between the two different electrodes increases the overall cell voltage that cannot be

negotiated [28]. Therefore an approach of amplifying specific capacitance in addition to cell voltage and pointing towards enhancing the performance is required. The case of increasing the specific capacitance is concerned with EDLC and pseudocapacitive electrodes while as the latter approach of increasing cell voltage is associated with hybrid supercapacitors [29]. This leads to a considerable betterment in performance and their respective applications.

The other approach consists of the development of nano-sized electrode materials to reduce the diffusion length and most importantly to provide higher outer layer area [30]. This approach is primarily concerned with supercapacitors and rechargeable batteries. Even the collaboration of the battery type and supercapacitor type electrodes forming hybrid supercapacitor resulted in increased energy density and higher voltages. The impactful factor is the recharging time of hybrid supercapacitors than the conventional lead-acid battery and other rechargeable batteries [31]. Currently, the main focus is towards getting the energy density of the hybrid supercapacitors in the range of 20–30 Wh kg<sup>-1</sup>.

## 2. Principles and mechanism of energy storage in supercapacitors

Presently there are various types of capacitors available for energy storage cataloged by means of specific dielectric used or by means of the capacitors physical state as shown in Fig. 2 [32]. Every capacitor displays its unique characteristics and applications varying from small trimming applications (normal capacitors) in electronics to high voltage power factor correction applications (supercapacitors) [33]. The research related to supercapacitors has enormously increased during the last few decades to fulfill the demand for applications requiring the properties like higher specific energy, better cyclic life, reliability etc.

Supercapacitors confronting electrochemical behavior have a similar configuration to the battery. Supercapacitor consists of bi-electrode configuration kept apart using a separator immersed in an electrolyte. The main constituents of the supercapacitor assembly are; two electrodes, electrolyte solution, separator and current collector as shown in Fig. 3. Supercapacitor characteristics are based on these constituents.

Supercapacitors are the type of capacitors in which energy storage is based on charging and discharging processes at the electrode-electrolyte interface [34]. The energy storage in supercapacitors is governed by the same principle as that of a conventional capacitor, however, are preferably appropriate for quick release and storage of energy [35]. In contrast to the conventional capacitor, supercapacitors possess incorporated electrodes having a greater effective surface area which leads to enhancement in capacitance by a factor of 10 000 than conventional capacitors [36]. While conventional capacitors storage is in range of micro to millifarads, the supercapacitor charge storage is in the

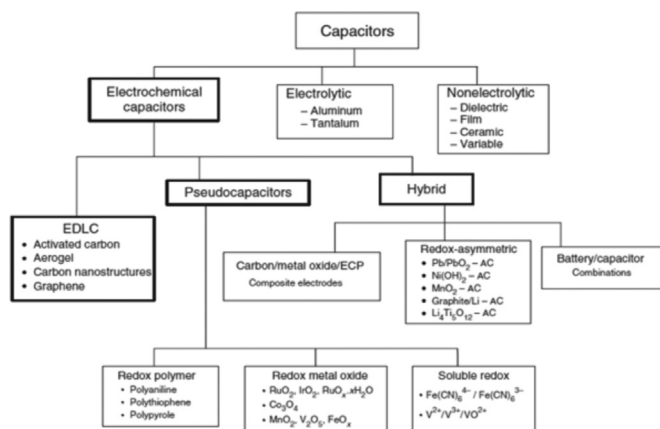


Fig. 2. Classification of capacitors. Reproduced with permission from Ref. [32]. Copyright © 2013 John Wiley and Sons.

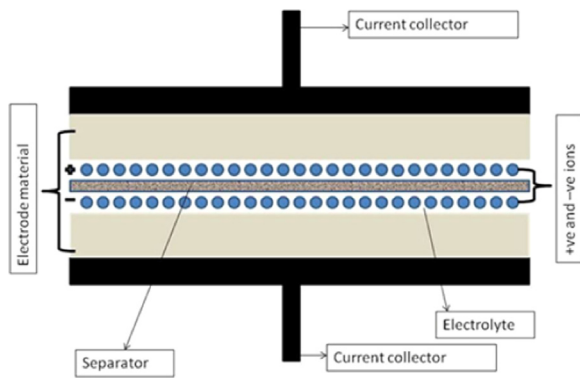


Fig. 3. Constituents of a supercapacitor.

range of 100–1000 F per device at the same time maintaining low equivalent series resistance and high operational specific power [37]. By means of proper designing of the supercapacitors, the range of specific energy and specific power can vary up to several orders of magnitude making supercapacitors flexible storage option.

The principles governing the energy storage is based on two mechanisms:

- The EDL capacitance due to adsorption of Coulombian charge near the electrode-electrolyte boundary.
- Pseudocapacitance owing to superficial redox reactions correlated to their respective potential.
- While collaboration of both forms the storage principle of the hybrid supercapacitor.

The storage mechanisms are mentioned separately for convenience.

### 2.1. Storage mechanism of an electric double layer capacitor (EDLC)

EDLC featuring capacitance mechanism is similar to a typical capacitance mechanism of dielectric capacitor [38]. In conventional capacitors, the capacitance is related to the separation between the two charged plates, tendering limited charge storage. However, a supercapacitor can store more energy based on EDL principle due to the large interfacial area of the electrodes with similar charge/discharge mechanism as that of the conventional capacitor. In EDLC charge is stored electrostatically due to reversible adsorption of ions of the electrolyte onto the electrochemically stable active material electrode [39]. The double layer capacitance is produced as a consequence of charge separation occurring due to polarization at the electrode-electrolyte interface. The charge storage takes place directly across the double layer of the electrode material without any charge transfer across the interface and hence the capacitance arises due to true capacitance effect. The surface charge generation mechanism takes place by means of dissociation of the surface, adsorption of ions from solution and defects in the crystal lattice of a material. The deficiency or excess of charge creation at the electrode surface leads to the creation of oppositely charged ions in the electrolyte near the electrode-electrolyte interface for electroneutrality. The thickness of the double layer is dependent on the electrolyte concentration and size of ions and is of order 5–10 Å for concentrated electrolytes.

Von Helmholtz in 19th century illustrated this type of charge storage mechanism while investigating opposite charge distribution at colloidal particles interface [40]. According to the Helmholtz model of charge storage in EDL; two layers of opposite charges are simultaneously formed maintaining separation equal to their atomic distance at the electrode-electrolyte interface [41]. However, the concept came into practical usage after 1957 as the EDLC patented by H.I. Becker of General Electric. The first kind of EDLC's consisted of porous carbon

electrodes immersed in an aqueous electrolyte. The electrodes were kept apart by an ion permeable separator [42].

The modification of the Helmholtz model was done by Gouy and Chapman, considering the distribution of the charge to be continuous along a layer in electrolyte solution termed as diffuse layer [43,44]. However, the limiting case for Gouy and Chapman model is a higher estimation of capacitance in EDL due to inverse correlation of capacitance with separation distance. Therefore, this model provides higher capacitance at the electrode's outer layer owing to the existence of ions near the electrode interface. Merging of two models corresponding to EDL mechanism was done by Stern in his EDLC model [45].

Stern's model explains the creation of bi-sections of ion allocation based on the binding of ions as inner section and outer sections termed as a compact layer (Stern layer) and diffuse layer respectively [46]. The Stern layer is composed of ions sturdily adhered on electrode whereas the diffuse layer is defined in accordance with Gouy and Chapman model containing continuous electrolytic ions distribution aided by thermal motion [47]. The distinction of ions in the compact layer is attained by dividing it into two planes called as inner Helmholtz plane in close proximity to the core of electrode and outer Helmholtz plane in contact with electrolyte [48].

The EDLC contains two electrodes adhered with the metallic current collectors. In addition to that, the electrodes are placed in an electrolyte solution with ion permeable separator in the center. The purpose of the separator is to avoid short circuit. The parameter determining capacitance in EDLC is the width of the binary layer at the electrode-electrolyte boundary, which is much smaller compared to the thickness of the separator. The capacitance is measured in correspondence to the general capacitance equation [49].

$$C = \frac{A \times \epsilon_0}{d} \quad (1)$$

Where  $C$  denotes the capacitance measured in farads,  $A$  denotes surface area,  $\epsilon_0$  denotes permittivity of free space and  $d$  denotes effective width of the electric double layer also termed as Debye length.

The outcome of energy in a normal EDLC is reliant on electrostatic attraction among the ions at electrode and electrolyte contact [50]. The schematic illustration of an EDLC capacitor is shown in Fig. 4 [51]. The configuration of an EDLC is simple in which two electrodes are immersed in an electrolyte kept apart by a separator.

Currently, there exists a wide range of EDLC materials, each material showing its unique characteristics that significantly impact the performance of the device. The selection of electrode material is essential in determining the electrical properties. The charge storage due to double layer mechanism is a surface process and therefore the

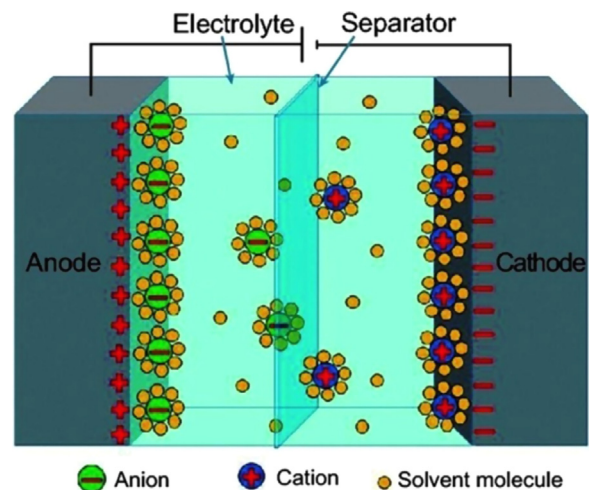


Fig. 4. Schematic representation of an EDLC. Reproduced with permission from Ref. [51]. Copyright © 2017 Elsevier.

surface characteristics of the electrode material produce a significant impact on the capacitance. Among various materials showing EDLC behavior, carbon has been used since the development of supercapacitors due to its high surface area. Even in current times, carbon remains the most explored EDLC electrode material due to its low cost, availability and its ability to exist in different manufacturing forms like nanotubes, fibers and foams. The transformation of carbon into an activated form like activated carbon impacts on the porosity and their accessibility of pores to the electrolyte. It is essential to point out that the ion mobility within pores is completely different from ion mobility in the bulk of the electrolytic solution. But the pore size produces a significant influence on the overall ion mobility in a cell.

Another noteworthy point to mention is the smaller size of pores allowing easy access to electrolyte does not contribute to the double layer capacitance. Therefore, it requires prime considerations regarding the pore size of the material suitable for the particular electrolyte to ensure optimization of pore size distribution upon the size of the ions. The advent of carbon nanotubes (CNTs) has opened new possibilities in the field of supercapacitors. The CNT tends higher capacitance values due to tangled networks with an open central canal [52]. Besides carbonaceous materials, attractive alternative electrode materials based on metal-oxides are vastly explored. The metal-oxide electrodes yield high specific capacitance and low resistance to enable construction of high energy and high power EDLCs. Among metal-oxides, the extensive research has been carried out on ruthenium oxide especially for military applications. The prototype cells containing ruthenium oxide as active material yielded an energy density of  $8.5 \text{ Wh kg}^{-1}$  and a power density of  $6 \text{ kW kg}^{-1}$  developed by the US Army Research Lab [53]. The limiting factor for ruthenium oxide in commercial applications is its cost and as such manganese oxide due to its lower cost and requirement of mild electrolyte makes it a feasible alternative. Manganese oxide comparatively provides lesser specific capacitance than ruthenium oxide. The various carbon and carbon-based materials used as EDLC electrodes in different electrolytes and their specific capacitance are summarized in Table 1.

AC based electrodes for EDLC show higher specific capacitance than all other forms after material optimizations promises a cheap, feasible and sustainable electrochemical capacitor followed by templated carbon. The energy density forms one of the vital parameters concerned with supercapacitor applications. The low energy density limits the use of EDLC in automobiles and other new storage devices [38]. The current energy density of EDLCs lies in the range of  $5\text{--}10 \text{ Wh}^{-1}$ .

## 2.2. Pseudocapacitor

Compared to the EDLC, pseudocapacitors show capacitance owing to redox reactions of faradaic nature enveloping the elevation of energy in pseudo-electrode [55]. Pseudocapacitance is completely non-electrostatic in nature and arises as a consequence of electrochemical charge-transfer accompanied by the finite amount of active material. Since the storage is based on redox reactions, pseudocapacitor is similar to a battery in its behavior to some extent [56]. The pseudocapacitor

along with the double layer forms a supercapacitor. In electrochemistry, the term pseudocapacitance designates a capacitive material of electrochemical nature with the linear reliance of charge stored on the width of the potential window [57]. The charge storage initiates from diverse reactions. The pseudocapacitance occurs at the electrode surface where the faradaic charge storing mechanism applies [58]. In pseudocapacitor, there is involvement of charge passage across double layer with capacitance related to the amount of charge accepted and varying potential.

The pseudo electrodes are mainly comprised of oxides of metals, carbon doped with metal and polymers owing conductive property. The pseudocapacitance ( $C$ ) is given by the derivative of charge acceptance ( $\Delta q$ ) and changing potential ( $\Delta V$ ) that is

$$C = \frac{d(\Delta q)}{d(\Delta V)} \quad (2)$$

The differentiating factor between EDL and pseudocapacitor is that pseudocapacitor engrosses swift and reversible redox reactions experienced amidst the active material on electrode and electrolyte interface. The reason for redox reactions is of thermodynamic nature [59]. The schematic illustration of a typical pseudocapacitor is shown in Fig. 5 [51].

The capacitance arises in pseudocapacitor electrodes on the application of potential which induces a faradaic current from reactions like electrosorption or redox reactions of the electroactive materials like  $\text{RuO}_2$ ,  $\text{Co}_3\text{O}_4$ , etc. The process of electrosorption takes place due to chemisorption of electron donating anions like  $\text{Cl}^-$ ,  $\text{B}^-$ , etc. The electrosorption reaction of anions at the electrode surface along with  $\delta e^-$  contribute electrosorption valence [51]. Contrary to that, the redox reactions take place due to charge exchange across the double layer instead of a static separation of charge. Both EDLC and pseudocapacitor charge mechanisms exist in an electrochemical capacitor, however, based on the materials; one storage mechanism becomes the dominant contributor to the specific capacitance while the other contributes very little. Generally, metal oxides like; ruthenium oxides [60], vanadium nitride [61], manganese oxide [62], conducting polymers such as polyaniline (PANI) [63], carbon-based hetero-atoms [64–80], other transition metal oxides [81–92] and nanoporous carbons with electro-sorbed hydrogen show pseudocapacitance [93–98]. The specific capacitances of different pseudocapacitive materials including transition metal-oxides and conducting polymers are summarized in Table 2.

Pseudocapacitance is higher than EDLC, but their poor electrical conductivity leads to a deficiency of cycling stability and low power density. The capacitance is 10–100 times more than normal EDLC [82]. The pseudocapacitance exists as a consequence of faradaic charge shift of reversible redox reactions besides intercalation and de-intercalation processes like in batteries [83]. Pseudocapacitor includes metallic current collectors glued to the electrodes, which are placed in an electrolyte solution with separator [84]. In pseudocapacitor, the electrode potential is combined with the charge storage of electroactive species (electro-adsorbed) to give a continuous logarithmic function of the extent of sorption [98,99]. Hence, pseudocapacitor electrodes show

**Table 1**  
Summary of various EDLC electrode materials.

Electrode materials	Electrolyte	Capacitance ( $\text{F g}^{-1}$ )	Refs.
AC	Aqueous (NaOH/KOH)	200–400	[51]
Templated carbon	Aqueous (NaOH/KOH)	120–350	[52]
CNT	Aqueous (NaOH/KOH)	20–180	[53]
Carbide-driven carbon	Ionic liquids (KCl/NaCl)	100–150	[51]
Carbon black	Aqueous (NaOH/KOH)	< 300	[51]
Carbon Aerogels/xerogels	Aqueous (NaOH/KOH)	40–200	[52]
Graphite and reduced Graphene oxide (rGO)	Tetraethylammonium tetrafluoroborate ( $\text{Et}_4\text{NBF}_4$ )	10–150	[54]
Mesoporous carbon	KOH	180	[55]
AC fibers	KOH	180–210	[56]



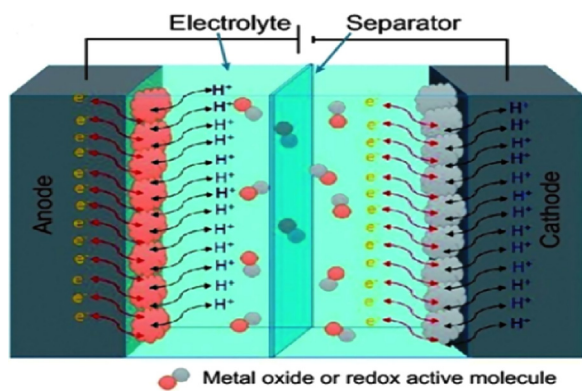


Fig. 5. Schematic diagram of a pseudocapacitor. Reproduced with permission from Ref. [51]. Copyright © 2017 Elsevier.

a linear dependence of charge stored to the charging potential. This linear dependence results in charge storing mechanism based on electron transfer instead of the charge accumulation of the ions in EDLC [100]. Pseudocapacitance does not exist without double layer capacitance [101].

The transition metal oxides for pseudocapacitance explored significantly to enhance the parameters like long-term cyclability. Since, the transition metal-oxides especially  $\text{RuO}_2$ ,  $\text{Fe}_3\text{O}_4$ ,  $\text{MnO}_2$ , etc undergo fast and reversible redox reactions, it especially requires optimizations related to cyclability. Among the transition metal-oxides the most explored material is  $\text{RuO}_2$  due to its ideal capacitive behavior, theoretically capable of yielding pseudocapacitance of greater than  $1300 \text{ F g}^{-1}$ . But as per recent reports, the maximum specific capacitance of  $720 \text{ F g}^{-1}$  has been achieved [60]. The reasons for high capacitance yield are its high electrochemical reversibility and extensive cyclability. In  $\text{RuO}_2$  the charge storage occurs in aqueous electrolyte due to electrochemical protonation showed in reaction [102]:



where  $0 \leq \delta \leq 1$  over a voltage window of  $\sim 1.2 \text{ V}$ .

As per reports by McKeown et al. [103]  $\text{RuO}_2$  in hydrous form exhibits a higher specific capacitance of  $\sim 720 \text{ F g}^{-1}$  while yields specific capacitance of  $\sim 350 \text{ F g}^{-1}$  in acidic electrolytes. The reason as per McKeown et al., behind high specific capacitance yield, is its high protonic and electronic conductivity facilitating redox reactions of electrochemical nature in  $\text{RuO}_2$ . The hydrous  $\text{RuO}_2$  following the symmetric pseudocapacitor configuration yielded maximum specific

capacitance of  $734 \text{ F g}^{-1}$  in  $1 \text{ M H}_2\text{SO}_4$  electrolyte with specific energies of  $25 \text{ Wh kg}^{-1}$  and  $12 \text{ Wh kg}^{-1}$  at a specific power of  $92 \text{ W kg}^{-1}$  and  $21 \text{ W kg}^{-1}$  [103]. The other transition metal-oxides like  $\text{PbO}_2$ ,  $\text{NiO}$  and  $\text{MnO}_2$  have shown similar trends in aqueous and acidic electrolytes. The specific capacitance of these metal-oxides was comparatively lower to that of  $\text{RuO}_2$  in respective electrolytes [90]. The pseudocapacitance arises in such metal oxides due to proton insertion and de-insertion [104]. The causes for comparatively less pseudocapacitance with respect to  $\text{RuO}_2$  in such metal-oxides is due to limited surface layering and difficulty in cationic or protonic diffusion in bulk due to the partial utilization of active material. However, proper material optimizations like increasing surface layering can lead to specific capacitance enhancement in such metal-oxides.

Contrary to transition metal-oxides, conducting polymers show relatively more specific capacitance and among conducting polymers PANI is the more explored one. PANI due to its ease of preparation (chemical or electrochemical), better electrical conductivity ( $0.1\text{--}5 \text{ S cm}^{-1}$ ), high level of doping ( $\sim 0.5$ ) and environmental stability, display higher specific capacitance values [105]. PANI prepared by chemical method shows specific capacitance of  $200 \text{ F g}^{-1}$  while PANI prepared by electrochemical method displays specific capacitance of greater than  $1500 \text{ F g}^{-1}$  [63]. The variation in capacitance due to the preparatory method is directly related to the morphology and electrode thickness [106]. The highest capacitance for PANI is achieved in aqueous acidic electrolytes due to the requirement of proton charging and discharging when prepared by the electrochemical method. The other conducting polymers showing electrochemical activity yield specific capacitance lesser than that of PANI.

The essential aspect of Faradaic reactions to occur is the diffusion factor related to voltage [107]. Such reactions involve de-solvated ions having a smaller size than solvated ions [108]. The amount of pseudocapacitance obtained is due to the potential extent of the coverage area of adsorbed ions as a linear function within a shorter limit [109]. The electrode's chemical affinity related to adsorption on the surface, structure and pore dimensions, also plays a vital role in yielding pseudocapacitance [110]. Not only does pseudocapacitance arise from redox reactions, but also some chemisorption reactions of electrolyte material yields pseudocapacitance [111–113]. Therefore, it is essential to optimize the pseudocapacitive electrode material to provide beneficial redox sites, leading to increasing the specific capacitance. Among the reported materials for pseudocapacitors;  $\text{RuO}_2$  and PANI display highest specific capacitance values.

Table 2

Summary of different pseudocapacitive electrode materials.

Electrode material	Electrolyte	Specific capacitance ( $\text{F g}^{-1}$ )	Refs.
$\text{RuO}_2$	$\text{H}_2\text{SO}_4$	650–735	[60]
$\text{MnO}_2$	$\text{K}_2\text{SO}_4$	261	[82]
$\text{Ni(OH)}_2$	KOH	578	[83]
$\text{MnFeO}_2$	PF6 (Hexafluorophosphate)	126	[84]
TiN	KOH	238	[85]
$\text{V}_2\text{O}_5$	KCl	262	[86]
Polyaniline (PANI)	Aqueous	120–1530	[63]
	Non-aqueous	100–670	
Polypyrrole (PPy)	Aqueous	40–588	[87,88]
	Non-aqueous	20–355	
Polythiophene (PTh)	Non-aqueous	1.5–6	[89]
Poly(3-methyl thiophene) (PMT)	Non-aqueous	20–220	[94,95]
	Ionic liquid	15–225	
Poly(3,4-ethylenedioxythiophene) (PEDOT)	Aqueous	100–250	[96–98]
	Non-aqueous	121	
	Ionic liquid	130	
Poly(4-fluorophenyl-3-thiophene) (PFPT)	Non-aqueous	10–48	[99]

### 2.3. Hybrid supercapacitor

The concept of hybrid supercapacitor came into existence as an effort to enhance the energy density to a range of 20–30 Wh kg<sup>-1</sup> [44]. These efforts were specially embarked on the enhancement of energy density criteria in EDLC thereby incorporation of either usage of better electrode and electrolyte material or by the development of hybrid supercapacitor. The hybrid supercapacitors formation results from coupling of different redox and EDLC materials like graphene or graphite, metal oxides, conducting polymers and activated carbon [114–117]. The coupling approach was put forward to overshadow the energy density factor of conventional EDLC's and pseudocapacitors thereby employment of hybrid systems consisting of the battery (faradaic) like electrode and capacitor (nonfaradaic) like electrodes [118]. The combination has higher working potential and yields higher capacitance which is two to three times more than that of conventional capacitors as well as EDLC and pseudocapacitors.

Hybrid supercapacitors storage principle is governed by a combination of the EDLC and pseudocapacitor storage principles. The limiting property of EDLC is not present in the pseudocapacitor and vice versa, their combination together leads to overshadowing of the limitations of the combining components, with an advantage of delivering higher capacitance. Hybrid supercapacitors are either symmetric or asymmetric depending upon the configuration of the assembly. The schematic diagram of a hybrid supercapacitor composed of Li insertion electrode and carbon electrode is shown in Fig. 6. Hybrid supercapacitors, when composed of two different electrodes made of different materials show better electrochemical behavior than the individual ones. Hybrid systems maintain the cycling stability and extent of affordability which are the limiting consequences in the achievement of success in the pseudocapacitor [116]. In contrast to the symmetrical EDLC, the hybrid type has extended values of specific capacitance besides higher rated voltage analogous to higher specific energy.

The assembly of two similar supercapacitor electrodes is the symmetric hybrid supercapacitor comprising of similar EDLC and pseudocapacitive components. The commercially available symmetric hybrid assembly comprises of binary electrodes of AC inside organic electrolyte with an operational potential up to 2.7 V [119]. The assembly of two dissimilar electrodes forms the asymmetric hybrid supercapacitor and most widely used asymmetric hybrid supercapacitor are the AC and MnO<sub>2</sub> along with AC-Ni(OH)<sub>2</sub> [120]. All the commercially available hybrid supercapacitors are asymmetric and those with conducting polymer electrodes are of prime interest [8]. In conducting polymer based hybrid systems, the conducting polymers undergo redox reaction to store and release charge. During oxidation or doping, the ions are transferred to the polymer backbone and during reduction or dedoping; ions are transferred back to the solution. The charging as such

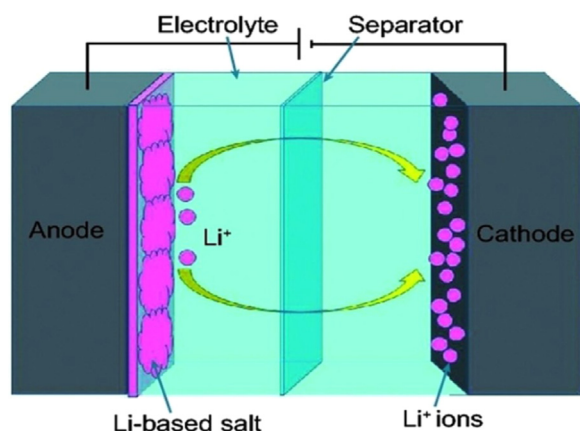


Fig. 6. Schematic diagram of a hybrid supercapacitor. Reproduced with permission from Ref. [51]. Copyright © 2017 Elsevier.

occurs along the bulk volume of the polymer matrix instead of along the surface as it is observed in carbon electrodes. The use of conducting polymers provides an opportunity to achieve higher specific capacitance. Mastragostino et al. [119] reported a prototype hybrid supercapacitor based on conducting polymer with specific capacitance of 39 F g<sup>-1</sup>.

The basic asymmetric hybrid supercapacitor consisting of the positive electrode of activated carbon (EDLC) united with Li<sub>4</sub>Ti<sub>5</sub>O<sub>12</sub> (Faradaic electrode) in an organic electrolyte was suggested by Amatucci's group [121]. The EDLC component supplies high power density while the pseudocapacitive component imparts the high energy density. Therefore dilapidation over the limitation of the incorporating components forms a hybrid component having uplifted parameters. Asymmetric assembly of activated carbon with potassium sulfate (K<sub>2</sub>SO<sub>4</sub>) and manganese dioxide (MnO<sub>2</sub>) has also been reported [122]. Most recently the advances of asymmetric supercapacitors were reviewed by Rajkumar et al. [123] in aqueous electrolyte. According to their report, for electrochemical performance enhancement, it is essential to study the physico-chemical properties and charge storage mechanism at the electrode-electrolyte interface. The improvement in energy density parameter can be attained by designing superior structures with good electronic conductivity, surface area and maximum electrochemically active sites for better ion transport. The hybrid supercapacitors with different electrode materials are summarized in Table 3. The variation in specific capacitance arises due to the nature of electrode material, electrolytes and fabrication technique.

The systematic advancement towards the classification of hybrid supercapacitors has been put forward by Cericola and Kötz comprising of the combinations of material [124]. According to them, not only EDLC and pseudocapacitor electrodes can form the hybrid supercapacitor assembly, but the incorporation of one such component with a battery type electrode is also a possibility. According to their proposal, hybrid systems can be symmetric or asymmetric depending on the electrochemical behavior and nature of electrodes implicated in the formation. On the one hand, the symmetric systems show superiority in comparison to the normal EDLC or a faradaic capacitor, but the asymmetric systems are exceptionally superior in all assets in comparison to the other types of supercapacitors. Hence, the best-suited system for supercapacitor is the asymmetric hybrid system.

The limitation of any supercapacitor restricting its ideal capacitive actions is the presence of internal resistance. The power performance of a supercapacitor is associated with its internal resistance which corresponds to the electrolyte resistance, current collectors and electrodes that are termed as equivalent series resistance (ESR) [125,126]. In comparison to EDLC; hybrid supercapacitors show lesser cyclability. The overall performance of hybrid supercapacitor is dependent on both electrodes as well as electrolyte material. It is important to choose the proper type of electrolyte for electrode materials for betterment in the overall performance of hybrid supercapacitor. The approaches to

Table 3  
Different hybrid supercapacitor electrode materials.

Electrode	Electrolyte	Specific capacitance (F g <sup>-1</sup> )	Ref.
Carbon/rGO	Na <sub>2</sub> SO <sub>4</sub>	175–430	[52,56]
RuO <sub>2</sub> /MWCNT	H <sub>2</sub> SO <sub>4</sub>	169.4 mF cm <sup>-1</sup>	[60]
MnO <sub>2</sub> /MWCNT	Na <sub>2</sub> SO <sub>4</sub>	141	[82]
MnO <sub>2</sub> /CNTA <sup>a</sup>	Na <sub>2</sub> SO <sub>4</sub>	144	[120]
rGO/MnO <sub>2</sub>	Na <sub>2</sub> SO <sub>4</sub>	60	[54]
PAN <sup>b</sup> /Carbon nanofibers	KOH	134	[99]
PANI/MWCNT	H <sub>2</sub> SO <sub>4</sub>	360	[63]
PPY/MWCNT <sup>a</sup>	H <sub>2</sub> SO <sub>4</sub>	200	[88]
PANI nanotubes/Titanium nanotubes	H <sub>2</sub> SO <sub>4</sub>	740	[115]

<sup>a</sup> MWCNT – Multiwalled carbon nanotubes, CNTA – carbon nanotube arrays, PAN – Polyacrylonitrile.

hybrid supercapacitors are discussed in Section 4.

### 3. Criterion for hybrid supercapacitor formation

The criterion for hybrid supercapacitor formation entails the parameters of energy and power. The models governing these parameters are the thermal and electric model. These criteria define the availability and number of devices to furnish the desired applications.

#### 3.1. Criteria of energy

An energy criterion determines the number of the devices adequate for providing energy parameter pertaining to elevated energy bound applications [127]. This involves following the procedure defined by the electric model of the supercapacitor. According to an electric model, the condition for maximum energy storage engrosses ignorance of relaxation constraints associated with the device [128]. In accordance with the electric model, the capacitance ( $C$ ) in such case is regarded as principal capacitance denoted by  $C_0$  [129]. This yields the maximum energy storage circumstances concerned with maximum voltage permissible for the device. The following equation gives correlation pertinent to maximum performance:

$$W_M = \frac{1}{2} C_0 V_M^2 \quad (4)$$

where  $W_M$  denotes maximum energy and  $V_M$  denotes maximum voltage.

To completely extort energy accumulated by a device, the voltage has to be descended to a minimum value ( $V = 0$ ) while using the device at maximum voltage. Conversely, current tends towards perpetuity at particular power when voltage drop heads on the way to zero. This restricts overall efficiency [130]. The losses concerned with ESR and interfacial resistance adds in restricting the overall efficiency [131]. The efficiency of the supercapacitor device as such is governed by the deviation of the voltage at the respective terminals. Therefore, another factor termed as discharge factor is introduced to apprehend on the minimum threshold voltage. This minimum threshold voltage is the limit of voltage below which supercapacitor forbids to discharge. The minimum threshold voltage is given in correspondence to a maximum voltage by the relation [132]:

$$d = \frac{V_m}{V_M} \times 100 \quad (5)$$

where  $d$  is discharged factor,  $V_m$  and  $V_M$  are minimum and maximum voltages respectively. The Eq. (5) demonstrates that there is no restriction on the number of devices in supercapacitor assembly which relies only on discharge factor [133]. For example, the symmetric hybrid supercapacitor composed of AC-AC yields an energy density of  $5\text{--}10 \text{ Wh kg}^{-1}$  when fabricated asymmetrically [52]. The device on the basis of its energy density tenders its promise in use for memory backups.

#### 3.2. Criteria of power

This criterion deals with the efficiency of the supercapacitor. There exists a limit at which power and the currents must be fixed to attain an efficiency of over 90% during charging and discharging for a hybrid supercapacitor. Considering the presence of low ESR, this extent of efficiency can still be accomplished [134]. To attain 90% efficiency, there exists an upper and lower limit for current and power while charging and discharging of a supercapacitor. The upper limit for current is set at 297 A and power is at 604 W while charging and lower limit for current is 267 A and power is 423 W while discharging [135]. The power density of hybrid supercapacitors ranges from 10 to  $1000 \text{ kW h kg}^{-1}$ . The power density parameter of  $806 \text{ W kg}^{-1}$  and efficiency of 90% was obtained by considering the lower limit of current

and power while the component mass kept at  $0.525 \text{ kg}$  [136]. These values are in contradiction with the values given by the makers according to whom for at same mass, limit of current and power, the power density is of order  $4300 \text{ W kg}^{-1}$  [137]. By consideration of efficiency parameter, the variations between the makers and observed values can be monitored while fabrication of supercapacitors [138]. For example, a supercapacitor composed of AC-Ni(OH)<sub>2</sub>, synthesized by hydrothermal route yields a power density greater than  $500 \text{ W kg}^{-1}$  [120]. The hybrid supercapacitor showed excellent cyclic performance on pre-treatment of active material before fabrication with ethanol. Hence, a power criterion forms an essential and decisive factor while considering the efficiency of a supercapacitor formation.

## 4. Hybrid supercapacitors components

### 4.1. Electrode materials

Generally, hybrid supercapacitors mostly with enhanced performance are a combination of two electrodes, the first one being supercapacitor electrode and another one being battery electrode [139]. To achieve higher capacitance values, mainly three approaches are considered [118];

- By using an electrode materials with higher capacitive properties.
- By variation of electrolytes.
- By development of hybrid capacitors.

There are numerous possibilities for the formation of hybrid systems resulting from the combination of different capacitive materials with the uniqueness of certain capacitive characteristics [140]. Hybrid electrodes are classified as composite, battery type and asymmetric as shown in Fig. 7.

The classification of hybrid electrodes is on the basis of dominant electrode behavior. The hybrid assembly constituting of composite electrodes comprises of incorporated carbon to either conducting polymers or metal oxides [141]. Hence, it enables mutual charge storage pertaining to physical and chemical means together in an electrode. The EDLC part is played by the carbon materials thereby providing a capacitive double layer and greater surface area for capacitance [142]. Whereas, metal oxides or conducting polymers behave as pseudocapacitors. The greater surface area feature pertains to the enhancement of contact among the engulfed pseudo-material and the electrolyte. The second class of hybrid supercapacitors comprises of two different materials with redox properties while the third type of supercapacitor contains battery type material electrode and supercapacitor electrode. The types of hybrid supercapacitors on the basis of configuration and electrode materials are discussed in the next section.

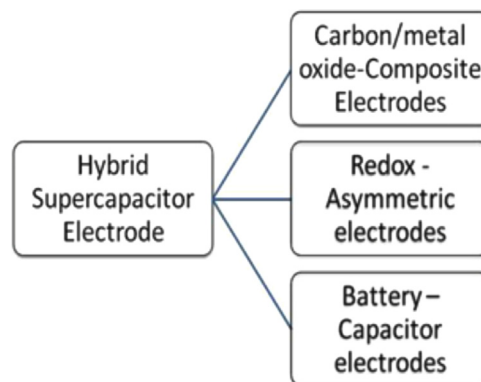


Fig. 7. Classification of hybrid electrodes.

#### 4.1.1. Asymmetric and symmetric hybrid systems

The asymmetric hybrid capacitor systems are developed, in order to improve energy and power density of electrochemical capacitors. The asymmetric hybrid system incorporates the advantages of long-term cycling and reversible non-faradaic negative electrode and a high capacitive positive electrode to accomplish requirements related to high energy and power density [143,144]. The common example of an asymmetric hybrid assembly is the activated carbon and conducting polymer [145]. The configuration is similar to that of composite electrodes containing activated carbon as negative electrodes while the conducting polymer as a positive electrode. The conducting polymer as pseudocapacitor electrode displays limited performance. However, utilization of such materials in an asymmetric hybrid capacitor elevates the efficiency to some extent and yields elevated power and energy density in addition to improved cycling stability [146].

The comparison between asymmetric and symmetric hybrid supercapacitors is based on the nature of the electrode material. In symmetric hybrid supercapacitor, the electrodes are inherited of same materials, while the electrode materials are itself in the hybrid form [147]. The example of the symmetric hybrid supercapacitor is PANI- PANI with each electrode having a different mass concentration of PANI. The symmetric supercapacitor characteristics can be acquired by consideration of single electrode also. In contrast, an asymmetric hybrid supercapacitor is composed of electrodes of dissimilar material. Each electrode has an impact on overall characteristics of the supercapacitor. In the asymmetric system, the supercapacitor behavior is subjective to each electrode's operational voltage which restricts the individual characteristics of each electrode while measurements. The electrochemical behavior encompasses the entire supercapacitor cell as a whole instead of the individual electrode in asymmetric design [148]. The example of an asymmetric system is Mn-Ni-Co (MNCO) ternary oxide along with carbon black. The schematic asymmetric cell is showed in Fig. 8 composed of stainless steel with spring, metal plates, cathode and anode material along with separator [149].

The asymmetric system formed by MNCO ternary oxide along with carbon black was synthesized by hydrothermal method forming nano-wire structure [150]. The synthesized material displayed excellent performance due to the large surface area for faradaic reactions and rapid ion transfer. This asymmetric system is shown in Fig. 9 with MNCO as positive electrode and carbon black as a negative electrode. The comparison between the carbon-carbon symmetric capacitor and MNCO and carbon black is portrayed in the Ragone plot. Clearly, it is evident that asymmetric systems display better performance than the symmetric ones.

A similar type of results was reported in case of  $\text{MnO}_2$ -PEDOT and rGO-CNT asymmetric hybrid cell system [149]. The hybrid structure was synthesized by controlling the critical kinetic factors (temperature and pressure) during vapor deposition polymerization, leading to the formation of multidimensional polymer nanostructures. The multi-dimensionality in the structure was obtained by core etching process. The

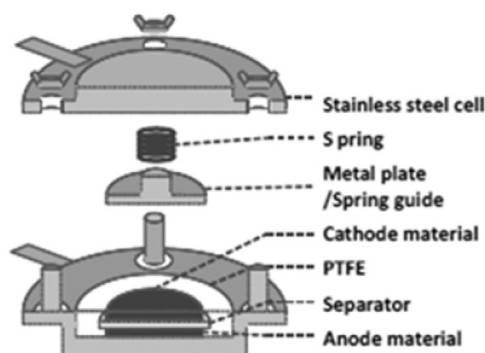


Fig. 8. Schematic representation of asymmetric cell. Adapted from Ref. [149].

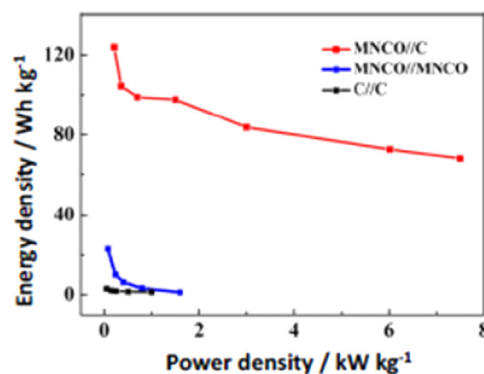


Fig. 9. Ragone plots displaying performance of the asymmetric MNCO-carbon black, symmetric MNCO//MNCO and symmetric carbon-carbon capacitors. Reproduced with permission from Ref. [150]. Copyright © 2014 American Chemical Society.

pseudocapacitance in this hybrid system arose from  $\text{MnO}_2$ -PEDOT (positive electrode) while rGO-CNT acted as an EDLC (negative electrode). PEDOT provides a larger effective surface area and quick ion transfer due to the nano-scale hierarchical structure. In the asymmetric structure, CNT was incorporated between rGO sheets, to avoid sheet restacking thereby increasing the non-faradaic charge storage. This asymmetric combination of  $\text{MnO}_2$ -PEDOT (+) and rGO-CNT (-) system revealed superior specific capacitance, cycling stability, and columbic efficiency. The asymmetric structure at the weight ratio 1:1 showed a specific capacitance of  $153 \text{ F g}^{-1}$  in an acidic electrolyte.

#### 4.1.2. Hybrid systems containing battery type electrodes

The battery type hybrid assembly is composed of an amalgamation of two diverse electrodes [151]. This type offers a pairing of a supercapacitor electrode to a battery type electrode [152]. The escalating energy feature is portrayed by supercapacitor electrode while elevated power is characteristic of the battery electrode [153]. The battery type materials are the ones which undergo faradaic redox reactions during charging and discharging while materials undergoing charging and discharging following double layer capacitive procedure are the supercapacitor type.

The supercapacitor materials include porous carbons, graphene, oxide compounds, conducting polymers, intercalated lithium compounds [154,155]. The supercapacitor combination with Li-ion storage systems is of greater significance due to the presence of highest energy density in Li-ion. The energy density of Li-based systems ranges from 120 to  $200 \text{ Wh kg}^{-1}$ . Since supercapacitors possess the highest power density ranging from 2 to  $5 \text{ kW kg}^{-1}$  or even more. The combination of these two parameters works as an enhancing feature in hybrid supercapacitor formation. One such combinational product was developed by Telcordia technologies named as nonaqueous asymmetric hybrid [156].

The overview of components used by Telcordia technologies displayed in Fig. 10 comprises of activated carbon and lithium intercalated devices devoted to electrochemical storage [154]. This hybrid combination presents the advantage of integrating high energy density and high power density from its Li-ion battery component and supercapacitor component respectively. The hybrid assembly uses  $\text{Li}_4\text{Ti}_5\text{O}_{12}$  as anode featuring high power capability and excellent cycle life allowing Li-ion intercalation devoid of Li plating while using highly conductive acetonitrile-based electrolyte [154,157]. This anode is coupled with activated carbon acting as double layer capacitive or positive electrode. As a consequence of coupling, the resulting device has charge storage behavior of battery at the negative electrode and charge storage behavior of supercapacitor at the positive electrode. Besides activated carbon, the other positive electrodes used for such hybrid devices include  $\text{LiCoO}_2$  or  $\text{LiMn}_2\text{O}_4$  forming a high power hybrid Li-ion battery [158].



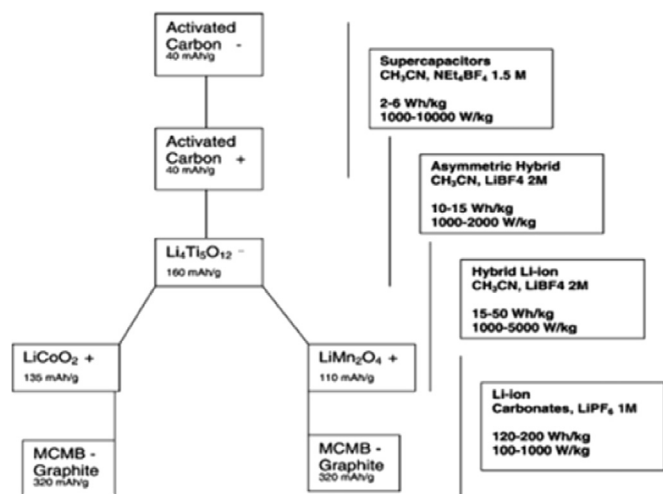


Fig. 10. Overview of the components used in the family of electrochemical storage devices developed by Telcordia Technologies. Reproduced with permission from Ref. [154]. Copyright © 2003 Elsevier Science B.V. All rights reserved.

The electrode materials in Fig. 10 along with their coupling possibilities are listed with their energy and power densities. Clearly, the hybrid Li-ion coupled systems exhibit the most energy and power density followed by asymmetric and supercapacitor systems [154]. In the battery type hybrid systems, the anodic pseudocapacitor electrodes are developed from  $\text{RuO}_2$ ,  $\text{MnO}_2$ ,  $\text{V}_2\text{O}_5$ ,  $\text{PbO}_2$ ,  $\text{Co}_3\text{O}_4$ ,  $\text{Ni}(\text{OH})_2$ ,  $\text{NiO}$ ,  $\text{Co}(\text{OH})_2$ ,  $\text{Fe}_3\text{O}_4$ , few hydroxides like  $\text{Co}(\text{OH})_2$  and  $\text{Ni}(\text{OH})_2$  [159] along with conducting polymers [160]. These pseudocapacitive electrodes are combined with the capacitive carbon-based materials like activated carbon and CNTs possessing high porosity [161–165]. Their combination with graphene also forms the asymmetric hybrid assembly as per reports [166–168]. The anodic pseudocapacitor electrodes show capacitance upto  $700 \text{ F g}^{-1}$  [169–174]. The capacitance of the carbon-based materials is upto  $300 \text{ F g}^{-1}$  [175]. Therefore overall capacitance values are in the range of  $650\text{--}1000 \text{ F g}^{-1}$  leading to the formation of hierarchical asymmetric hybrid supercapacitors [176]. However, the electrolytes can be aqueous and non-aqueous in nature. Considering the report by Brousse et al. [177] on nickel or cobalt-based electrode systems, the electrodes behave as pseudocapacitive electrodes instead of battery type electrode.

#### 4.1.3. Hybrid systems formed by coupling of EDLC and pseudocapacitive materials

The carbon coating on conducting polymers display exceptional cycling stability and tender better energy as well as power density [178]. The presence of carbon materials ensures the structural stability of pseudocapacitive conducting polymers [179]. On the other hand, the presence of conducting polymers ensures improvement in energy density [180]. The conducting polymers like PANI and PPy on coating with carbon material retained about 95% and 85% capacitance respectively in aqueous electrolyte after 10,000 cycles as reported by Liu et al. [181]. The authors demonstrated enhancement of cycling stability by employing a simple strategy of depositing a thin carbonaceous shell onto conducting polymer surface. This technique can be used in the fabrication of stable polymer electrodes incorporated with carbonaceous materials. The relation between capacitive retention and wave number termed as cycling performance of carbon material (C) and conducting polymers (PANI and PPy) is shown in Fig. 11. The cyclic voltammetry (CV) plots are also inserted in Fig. 11(a) and (b) to display the difference in capacitance in conducting polymers (PANI and PPy) and conducting polymers with the carbon materials.

#### 4.1.4. Hybrid systems formed by various electrode materials

The hybrid components comprising of various components are listed in Fig. 12. The classification of hybrid component materials consists of carbon materials, inorganic materials and conducting polymers. The carbon-based materials include activated carbon, CNTs, carbon aerogels and graphene [170]. The inorganic materials include manganese oxide and lithium-based materials while conducting polymers include polymers like PEDOT, PANI, PPy etc. [181,182]. The examples of hybrid electrode materials are the activated carbon-cobalt oxide, activated carbon-nickel oxide. In recent investigations, activated carbon-lead oxide is considered as the best hybrid system owing to its low cost and elevated voltage (2 V) in hydrous electrolyte [122]. This hybrid system delivers exact capacitance of  $71.5 \text{ F g}^{-1}$  and specific energy of  $32.2 \text{ Wh kg}^{-1}$  at discharging current density of  $200 \text{ mA g}^{-1}$  and 0.8–1.8 V potential range respectively [122].

The explicit problems in battery and capacitor can be compensated in the hybrid supercapacitor. Prior to that association of AC electrodes alongside positive faradaic electrodes like manganese dioxide ( $\text{MnO}_2$ ) in an aqueous electrolyte has been successfully tested for the hybrid device approach. The corresponding examples of such systems include AC-Ni ( $\text{OH})_2$  [123], AC- $\text{Li}_4\text{Ti}_5\text{O}_{12}$  [124], AC-graphite [125], AC- $\text{LiMn}_2\text{O}_4$  [182], AC- $\text{PbO}_2$  [183] etc. The energy and power density features of such hybrid systems are mentioned in Table 4.

Hybrid materials composed of carbon nanofibers (CNF) along with  $\text{MnO}_2$  form the low-cost supercapacitor. The design being core-shell (Core-CNF, Shell- $\text{MnO}_2$ ) provides high conductivity with an effective electrical connection between the core and the shell [184]. Another common hybrid assembly includes a combination of hydroxide with reduced graphene oxide (RGO). The positive electrode is either  $\text{Co}(\text{OH})_2$  or  $\text{Ni}(\text{OH})_2$  while the negative electrode is RGO [185]. The Ni ( $\text{OH})_2$ -RGO yielded specific energy close to  $30 \text{ Wh kg}^{-1}$  corresponding to power density of less than  $1 \text{ kW kg}^{-1}$ . The other hybrid composition of  $\text{Co}(\text{OH})_2$ -RGO yielded much lower values of power as well as energy compared to Ni( $\text{OH})_2$ -RGO.

The other examples of asymmetric hybrid supercapacitors with activated carbon as one electrode are AC- $\text{MnO}_2$  [186], AC-NiO, AC- $\text{Li}_2\text{Mn}_4\text{O}_9$ , AC- $\text{LiTi}_2(\text{PO}_4)_2$ , AC- $\text{Li}_4\text{Ti}_5\text{O}_{12}$  with aqueous electrolytes [187]. The asymmetric assembly of AC- $\text{MnO}_2$  in  $\text{K}_2\text{SO}_4$  electrolyte operated at a potential range of 0–1.8 V furnishes  $17 \text{ Wh kg}^{-1}$  of energy and  $2 \text{ kW kg}^{-1}$  of power [188]. The most common materials flourishing the hybrid supercapacitors are the composite materials consisting of carbon material with either oxide of metals or polymers possessing conducting property covering the features of combined double-layered capacitor and pseudocapacitor.

Besides this, manganese dioxide ( $\text{MnO}_2$ ) has been widely used for energy storage as a single electrode as well as for hybrid electrodes [189]. Some of the  $\text{MnO}_2$  based hybrid systems include  $\text{NiMoO}_4$  nanowire @  $\text{MnO}_2$  core-shell designed hybrid material yielding the areal capacitance values  $3.90\text{--}3.22 \text{ F cm}^{-2}$  at current densities  $8 \text{ mA cm}^{-2}$  and  $24 \text{ mA cm}^{-2}$  respectively while retaining its capacity after 4000 cycles [190]. Another hybrid material comprising of PPy and  $\text{MnO}_2$  with the incorporation of tungsten oxide ( $\text{WO}_3$ ) prepared by the electro-deposition method, having capacitance value ranging between  $11.38$  and  $14.21 \text{ F cm}^{-2}$  and specific capacitance of  $45 \text{ mF cm}^{-2}$  has been reported [191]. Spinel  $\text{Li}_4\text{Mn}_5\text{O}_{12}/\text{MnO}_2$  composite produced by the sol-gel method encompassing specific capacitance of  $53.3 \text{ F g}^{-1}$  corresponding to the current density of  $100 \text{ mA g}^{-1}$  with a range of working potential 0–1.3 V [192]. Apart from these, the interfacial polymerized PANI- $\text{PMo}_{12}$  hybrid material operated with the range of working potential of 0–0.75 V corresponding to the current density of  $1 \text{ mA cm}^{-2}$  produces a specific capacitance of  $68.82\text{--}172.38 \text{ F g}^{-1}$  depending on the increasing concentration [193]. Co-axial nanowire made by a network of silver molybdenum oxide core-shell as hybrid material gives specific capacitance of  $500 \text{ F g}^{-1}$  with an associated current density of  $0.25 \text{ A g}^{-1}$  [194]. Analogous to  $\text{MnO}_2$  some hybrid structures are graphene-based hybrid composites like  $\alpha\text{-MnMoO}_4/\text{graphene}$  composite

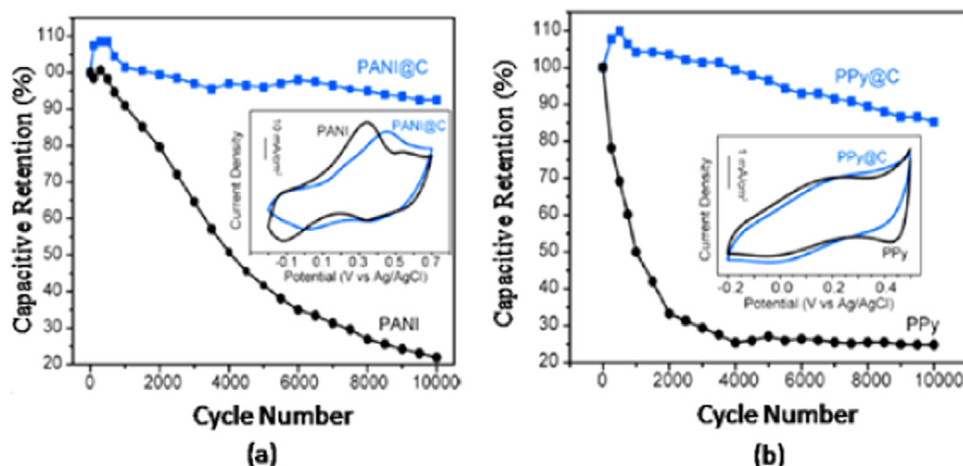


Fig. 11. Cycling performance along with cyclic voltammetry of (a) PANI (alone) and PANI@C electrodes and (b) PPy (alone) and PPy@C electrodes, collected at a scan rate of 100 mV/s in 1 M H<sub>2</sub>SO<sub>4</sub> electrolyte and CV at scan rate of 20 mV/s in 1 M H<sub>2</sub>SO<sub>4</sub>. Reproduced with permission from Ref. [181]. Copyright © 2014 American Chemical Society.

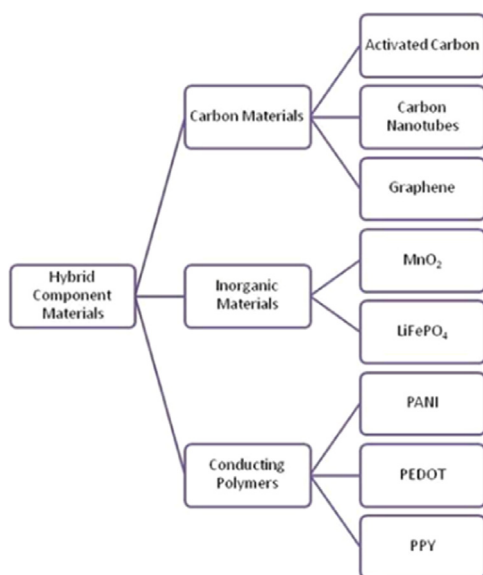


Fig. 12. Hybrid supercapacitor electrode component materials.

having a specific capacitance range of 234–364 F g<sup>-1</sup> associated with the current density of 2 A g<sup>-1</sup> and working potential range -1 V to +1 V with energy density range of 130–202.2 W h kg<sup>-1</sup> and the deliverance rate of 2000 W kg<sup>-1</sup> [195].

The combination of various electrode systems to form hybrid systems is still in the prospering state. Therefore, there are enormous opportunities to fuse the different type of electrodes to form a better hybrid system. Now not only the hybrid systems which are graphene-

based or activated carbon-based are investigated but also there is scope for a hybrid system containing metal oxides only or metal molybdates etc. The only concern is to choose the electrode for a particular behavior (either EDLC or pseudocapacitor). Also, there is an opportunity of combining two hybrid electrodes for better performance measures. These hybrid materials are synthesized using different synthesizing routes to deliver maximum efficiency related to their specific capacitance and provide sustainable means for energy storage to meet the energy demands in the modern era. Each type of hybrid supercapacitors provides its unique characteristics. The EDLC and pseudocapacitor based hybrid structure following a symmetric or asymmetric fabrication means provide an approach of combining the two storage principles. This combination yields specific capacitance in the range of 100–800 F g<sup>-1</sup>. Such hybrid supercapacitors are sufficient for the applications requiring low to medium power. On the other hand, the combination of supercapacitor electrode with a battery type electrode yields capacitance from 100 to 1000+ F g<sup>-1</sup> and can be useful in medium to high power applications. Clearly, the battery type hybrid supercapacitors have the edge over other combination of hybrid structures on all electrochemical parameters except cyclability. Therefore, it is essential to choose a suitable type of electrode material with respect to its applicability.

#### 4.2. Characteristic features of hybrid supercapacitors

The essential or the decisive characteristics related to hybrid supercapacitors progressive approach are the specific energy and power density along with other features like cycle life (charging-discharging cycles: self-discharging current along with coulomb's efficiency ( $\eta$ )) and energy efficiency [196]. The coulomb's efficiency ( $\eta$ ) determines the cyclic stability of the electrodes while comparing the initial and the final cycle and is given by the equation;

Table 4

Characteristic features and parameters of asymmetric and symmetric hybrid supercapacitors.

Electrode type	Supercapacitor	Working voltage (V)	Specific energy Wh kg <sup>-1</sup>	Power density kW kg <sup>-1</sup>	Refs.
Asymmetric EDLC + Pseudo = Hybrid	AC-AC	2.5–3.5	5–7	1–5	[172]
	Hybrid-Hard carbon- AC	2.2–3.8	10–30	1–10	[173]
	AC-LiMn <sub>2</sub> O <sub>4</sub>	0.5–1.8	5–10	0.1–1	[182]
	Ni(OH) <sub>2</sub> -AC	0.5–1.7	2–10	0.08–2	[123]
	AC-PbO <sub>2</sub>	0–2	10–30	0.05–1	[183]
	AC-Li <sub>4</sub> Ti <sub>5</sub> O <sub>12</sub>	2–3	5–20	0.1–1	[124]
	Graphite-AC	2–3.5	5–15	0.1–3	[125]
Symmetric Hybrid	PANI- PANI	0–0.5	3.13	10–10.9	[181]
	PPy-PPy	0–0.6	2.38	19–19.7	[181]
	PEDOT-PEDOT	0.0–6	1.13	23–23.8	[168]
	Carbon Maxorb-Carbon Maxorb	0–0.7	3.74	22–22.4	[173]

$$\eta = \frac{tD}{tC} \times 100 \quad (6)$$

where  $tD$  and  $tC$  are discharging and charging time respectively.

The specific power and the energy values of a supercapacitor are resolute of the charge-discharge method. There is an inverse affiliation of the significant parameters of supercapacitor related to power and specific energy determining the electrochemical behavior of the active species on the electrode [197]. The specific energy inherited by an electrode substance is given by the relation given in the equation:

$$E = \frac{1}{2} C_s (\Delta V) \quad (7)$$

where  $C_s$  is the specific capacitance in  $F\ g^{-1}$  and  $\Delta V$  is the cell voltage in V (volts) respectively. While the power of supercapacitor can be given by the equation as:

$$P = \frac{E}{tD} \quad (8)$$

where  $E$  is the energy and  $tD$  is the discharge time which is equal to  $tC$  (charging time) giving Coulombic efficiency following the equality of charge and discharge densities. The specific capacitance ( $C_s$ ) of an electrode material in a supercapacitor is obtained by employing the subsequent equation:

$$C_s = \frac{I}{dV/dt(w)} \quad (9)$$

where  $C_s$  denotes specific capacitance,  $w$  denotes total mass of the electrode,  $I$  is the average current in amperes (A) and  $dV/dt$  is the voltage scanning rate. The above equation is yielded from the CV plots of  $i$ - $E$  and  $E$ - $t$ ; that is current-energy and energy-time respectively. For ample amount of energy and power, the extent of capacitance ( $C$ ) and cell voltage ( $\Delta V$ ) go collateral which implies that both energy and power are directly proportional to  $C$  and  $\Delta V$  while the capacitance and voltage depend on the nature of electrode material along with the electrolyte [198].

#### 4.3. Electrolyte materials

In general, the electrolytes used in the supercapacitors are classified into two categories namely aqueous and non-aqueous [199]. The commercially available supercapacitors mainly consist of organic electrolytes which procure a wide range of cell voltage [200]. Considering the manufacturing consequence and the ease of unison, the asymmetric hybrid supercapacitors use the aqueous electrolytes possessing uplifted ionic conductivity [201,202]. Electrolytes play a pivotal role in supercapacitor performance. According to Burke, the operational voltage window variance arises due to the nature of electrolytes and its intrinsic resistance [124]. The square of the voltage window is proportional to the energy density whereas the power capability is inversely proportional to the ionic resistivity [203]. Currently, for hybrid supercapacitor, three categories of electrolytes are utilized namely aqueous, organic and ionic liquids [204].

The aqueous electrolytes like  $H_2SO_4$ ,  $KOH$ , and  $KCl$  are the most commonly used electrolytes due to their abundance and low cost. The capacitance does vary with the choice of electrolyte. The use of aqueous electrolytes gives enhanced specific capacitance but suffer from the limitation of restrictive voltage window [205]. The voltage window for aqueous electrolytes is only 1.2 V and any further increment to the voltage evokes consequences like the destruction of the cell through building pressure and water decomposition [206].

The organic electrolytes viable for supercapacitor application include acetonitrile and propylene carbonate due to their extent of operating voltage window. The organic electrolytes possess higher operating voltage than the aqueous electrolytes which is of the scale of 0–2.7 V [207]. This wider operational voltage range lifts the energy density to considerably higher extent than that of aqueous ones. Most

favorable organic electrolyte among the two mentioned earlier is acetonitrile because of its lower ionic resistivity while its toxicity and flammable properties limit its application [208].

The ionic liquids electrolytes are non-toxic, inflammable and have a broadest operating voltage range of 0–5 V [209]. The ionic liquid electrolytes are a liquid form of solvent-free molten salts at room temperature [210]. However, the ionic liquids have the limitation of insufficient ionic conductivity in reverence to the aqueous and organic electrolytes. The electrolyte has dual functionality in the system. Not only does it take part in conductance but also acts as a route for dissociation. The electrolyte imparts three kinds of influences to the system which are [211];

- The conductance of the electrolyte and the equivalent series resistance.
- Anion or cation adsorption based on the electrolyte.
- Determination of specific capacitance and its dependence on the potential of the double layer through dielectric features.

The intrinsic resistance  $R_e$  of the electrolyte acts as a buffer to put an increment to the charging and discharging speed of reversible processes [212]. Therefore presents instigation to highly porous electrode materials where the extent of contact between the porous electrode and the electrolyte must attain maximum surface. In the structure, the electrode's intrinsic resistance  $R_e$  arises because of inter-particle contacts which should be neglected [213]. One of the important affecting factors restraining the conductance of the electrolyte is the concentration of free charge carriers along with their ionic mutability. The concentration factor, in turn, is dependent on the degree of dissociation denoted by ' $\alpha$ '. The reduction in electrolyte resistance can induce maximum dissociation of the ions favorable for the accomplishment of the highest concentration of free mobile ions.

#### 4.4. Separator

The barrier functioning between the two electrodes is termed as the separator. It performs essential and cell sustaining functions. Inferior quality separators can impart negativity to the overall cell performance by stimulating additional resistance [214]. While in the worst case scenario, short circuiting of the whole cell is on the cards. Therefore, selection of separator is an important task ahead of the formation of the cell. The separators in inducement for hybrid supercapacitor task must satisfy the criteria as [215]:

- Separators must be non-conductive.
- They should infer minimum ionic resistance with electrolyte ion permeability.
- Induction of intrinsic resistance offered by chemical to the electrolytes and electrode materials.
- They should counter to the pressure and volume changes occurring in the cell by offering mechanical resistance. These changes may yield swelling of the cell.
- Separators should possess ease of wetting by the electrolyte.

The separators include material such as glass, paper, ceramics etc. [216]. Also, the polymer-based separators of low cost, porous nature and flexibility feature have been extensively used in supercapacitors. These polymer-based separators are classified as fibrous and monolithic separators. The polymeric separators used for supercapacitors are polypropylene, polypropylene-carbonate, polyvinylidene difluoride, polyethylene and polyamide [214]. Among these polymers, polypropylene is commonly used due to its ease of wettability. In another report, Graphene oxide (GO) has also been used as a separator [217]. The separator presence in supercapacitor ensures smooth ion transport without going under any chemical change. The polymer show most promising aspects regarding separator functionality due to their low

cost, processing simplicity, accessibility and very high mechanical and chemical resistance. However, the limitation arises on the basis of their wettability in different electrolytes and removal of moisture (mostly in polypropylene). To avoid these limitations, the surface modification of the polymer using plasma technology has been reported [218]. Besides the surface modifications by means of plasma technology, there are other possible modifications which can change the chemical and physical surface properties of the polymer like surface cleaning and improvement in wettability. As such the role of the separator is essential in determining the performance of a supercapacitor.

#### 4.5. Current collectors

Current collectors act as a complement to the performance of active materials with deficient conductivity. The current collector functions as a transporting medium of current from current source to the electrode and electrode to external load while performing the subsidiary function of heat dispersion generated within the cell [219]. In addition, recharging of the electrodes after use is also allied with current collectors. They are conductive electronically and endure tribulation in the cell conditions resisting chemical perversion from the electrolytes. The examples of current collectors are aluminum, steel, iron, and alloys etc. [220]. The coating of active materials into current collectors provides steadfast contact minimizes the interfacial resistance and raises the performance level [221]. This steadfast contact linking between the electrode and the current collector effectively minimizes the resistance arising due to the connection of heterogeneous materials.

The wide-ranging degree of cycling, the substantial delusion of the active material, the termination of electrode material and current collector leads to high resistance in the hybrid supercapacitor [222]. These limiting factors results in unfastening, diminishing and decent of material. As a consequence, the capacitance value decreases along with reduction in cycle life. Such scenario can be abstained by applying polymeric binding agents like Nafion and polytetrafluoroethylene, which restrains the disunion of the active material from the current collectors [223]. Also, another effective way of tackling this situation is to ensure best contact and processes implying surface treatment of collectors like imparting an additional conducting film with the binding agents [224]. This supplements the electrical conductivity and mechanical durability [225]. In recent times, nickel mesh, nickel foam, aluminum sheets etc have been used as current collectors. The active electrode materials are directly deposited on these conducting materials. In some cases, for better adhesion of active material with current collectors, a polymer acting as a binder is used. However, it is essential to choose to the suitable binding material, which can produce no consequences on the performance of the active material. An option of using conducting polymers as binders may result in improving the performance.

#### 4.6. Sealants

Sealants perform an auxiliary role in the hybrid supercapacitor assembly avoiding performance loss [226]. Sealant functions as a blockage to the outside contaminants like air, water, chemicals etc. These contaminations can bring about electrolyte degeneracy and surface oxidation on electrodes. Therefore, proper sealing of hybrid supercapacitor is a must. Unsuitable sealing can cause shunt resistance between the cells linked to the assembly. Shunt resistance can alter the overall efficiency of the system by stipulating other current paths [227]. Polymeric materials are mostly used as sealants due to their excellent features such as moisture resistance, flexibility etc. The proper sealing is often a hermetic seal based on the electrolyte material preventing entrance of gas and water in the cell. This type of sealing is applicable to the monopolar arrangement while as for bipolar arrangement better edge sealing is required to avoid passage of shunt current [228]. This shunt current leads to decent of charging efficiency and self-discharging

and also short-circuiting.

### 5. Assessment of electrochemical profile

The assessment of electrochemical profile deals with the determination of specific capacitance ( $\text{F g}^{-1}$ ), energy density ( $\text{Wh kg}^{-1}$ ) and power density ( $\text{W kg}^{-1}$ ) corresponding to specific current density ( $\text{A g}^{-1}$ ) [229]. These parameters yield the electrochemical performance of an electrode material in any supercapacitor assembly. The assessment of electrochemical profiling involves galvanostatic charge/discharge (GCD) test, CV characteristics and electrochemical impedance spectroscopy (EIS). These techniques are elaborated in upcoming sections.

#### 5.1. Galvanostatic charge/discharge assessment (GCD)

The evaluation of capacitance by GCD test is determined on the application of the equation:

$$C = \frac{I \times t}{\Delta V} \quad (10)$$

where 'C' represents differential capacitance ( $\text{F g}^{-1}$ ), 'I' is current density ( $\text{A g}^{-1}$ ), ' $\Delta V$ ' is the working potential window and 't' represents charging/discharging time (s) of the electrode. This test is one of the most efficient in the assessment of capacitance. In case of EDLC, there is no restriction on the range of potential window because of potentially independent charge storage but for intercalated pseudocapacitors or simple faradaic pseudocapacitors, the potential window range is always fixed [105,230]. Therefore, while capacitance determination of hybrid supercapacitors for EDLC part no fixation of potential window range is required but for the pseudocapacitive part potential window range has to be fixed depending upon the type of pseudocapacitive electrode [231]. The summation of the individual part capacitance then yields the total capacitance of the hybrid system. The GCD assessment yields criteria mentioned in the latter section. The GCD plot for  $\text{Co}_3\text{O}_4$  nanowire/nanoflower hybrid structure in 3M KOH solution is shown in Fig. 13 [232]. The hybrid structure was synthesized by a hydrothermal route using thermal treatment in air. The plot displays linear triangular shaped charge and discharge curves confirming the capacitance characteristics of the hybrid material [232]. From the GCD analysis of  $\text{Co}_3\text{O}_4$  nanowire/nanoflower hybrid structure, the capacitance values are in the range of  $4.8 \text{ mF cm}^{-1}$  to  $7.8 \text{ mF cm}^{-1}$  at a constant current density range of  $0.2\text{--}1.2 \text{ mA cm}^{-1}$ . In  $\text{Co}_3\text{O}_4$  nanowire/nanoflower hybrid structure, the results displayed the decrease in the current density from 61% to 58%.

GCD curve of another hybrid supercapacitor electrodes consisting of e- $\text{WO}_3$ /PPy and e- $\text{WO}_3$ /MnO<sub>2</sub> measured at a current density of  $1 \text{ mA cm}^{-2}$  is shown in Fig. 14 [191]. It is evident from the GCD curves that the e- $\text{WO}_3$ /MnO<sub>2</sub> hybrid supercapacitor displays higher specific

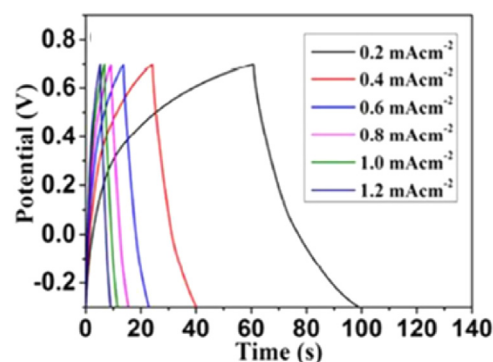


Fig. 13. Charge-discharge profile of  $\text{Co}_3\text{O}_4$ /CFC based symmetric supercapacitor. Adapted from Ref. [232].



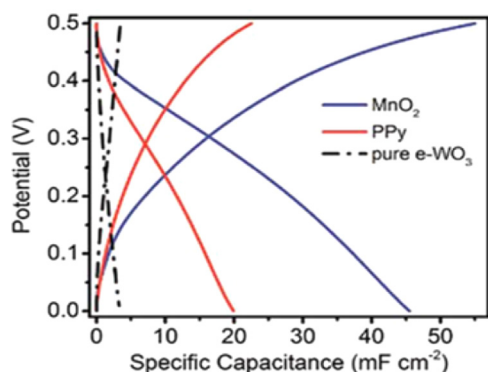


Fig. 14. GCD curves of the e-WO<sub>3</sub>/PPy and e-WO<sub>3</sub>/MnO<sub>2</sub> based hybrid supercapacitor measured at a current density of 1 mA cm<sup>-2</sup>. Reproduced with permission from Ref. [191]. Copyright © 2015 Royal Society of Chemistry.

capacitance of 45 mF cm<sup>-2</sup>, which is greater than PPy and pure e-WO<sub>3</sub> based supercapacitor [191]. The capacitive behavior of the hybrid device is confirmed by GCD curves at the charge/discharge rate of 1 mA cm<sup>-2</sup>.

#### 5.1.1. Material requirement

The material exhibiting symmetric curves during charging and discharging in addition to linear slopes revealing capacitance as a function of potential is said to be capacitive. To accomplish superior efficiency the mirror image curves relevant to charging and discharging ought to be sustained.

#### 5.1.2. Power determination

Power is determined by application of GCD curves as a function of the state of charge multiplied by the measured potential and applied current. This type of power determination is used in the construction of Ragone plots.

#### 5.1.3. Resistance calculation

ESR can also be determined from steady GCD curves. When the current direction is altered, an immediate descent in voltage (V) equal to twice the magnitude of the product of current (I) and resistance (R) that is:  $V = 2IR$ .

The resistance is calculated by using the same equation where current is the known quantity [225]. Besides current and voltage drop, the resistance is altered hugely by gas evolution like in over-oxidation of graphene films in carbon. The changes in resistance during such incidents are also visualized in GCD curves.

#### 5.2. Cyclic voltammetry

CV measurement is based on potentiodynamic electrochemical measurement. This analytic technique involves the electrode potential determination corresponding linearly to the time. In other words, electrode potential is plotted linearly versus time [105]. Also, the current versus applied voltage related to the working electrode is plotted which is called as cyclic voltammogram trace. The measurement is done by applying potential amid the working and the reference electrodes while the current is calculated amid the working and counter electrodes respectively. Hence, the assembly of three electrodes is required for CV measurements viz; working, reference and counter electrodes respectively. The rectangular curves give an appraisal of the capacitance of the electrode material by applying the equation;

$$C = \frac{I}{V} \quad (11)$$

where  $C$ ,  $I$  and  $V$  denote differential capacitance (F g<sup>-1</sup>), current density (A g<sup>-1</sup>) at the mean voltage and scan rate (V s<sup>-1</sup>) respectively. The cyclic voltammetry measurement on direct evaluation yield the average capacitance for both EDLC as well as pseudocapacitor based on the rectangular CV curve. While the battery type electrode or intercalated pseudocapacitor show redox peaks in the CV curves. Thus, no direct assessment of average capacitance is possible from CV curves [105].

CV analysis forms the basis for determining capacitance nature of a material. The typical CV curves of asymmetric Co<sub>3</sub>O<sub>4</sub> nanowire/

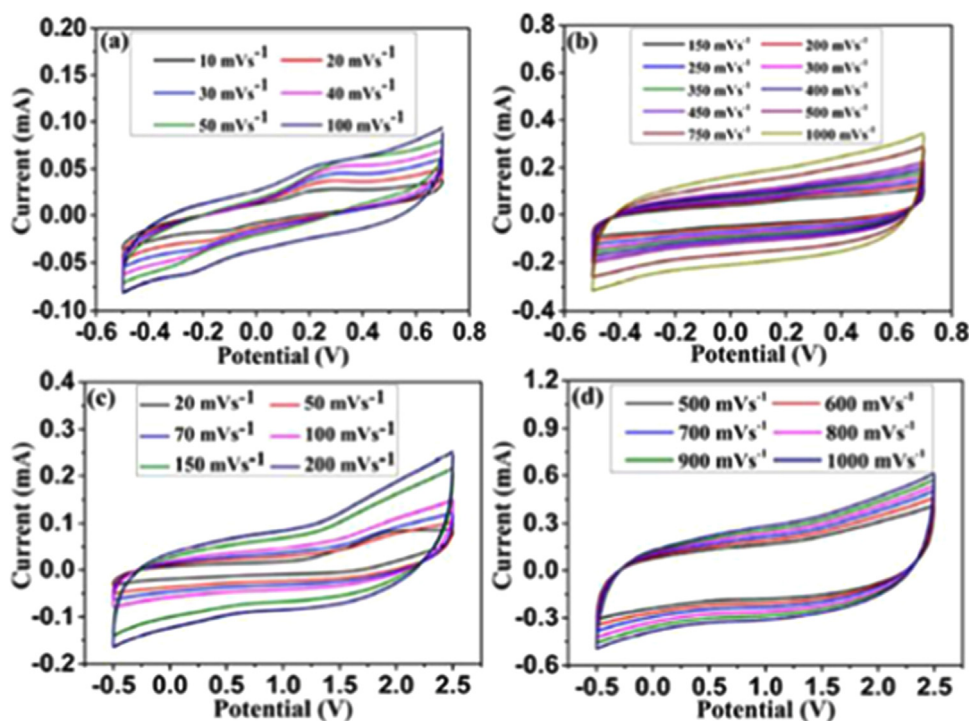


Fig. 15. Cyclic voltammograms of Co<sub>3</sub>O<sub>4</sub> based symmetric supercapacitor in 3 M KOH. (a and b) and 1 M TEABF<sub>4</sub> in PC (c and d) measured at different scan rates. Adapted from Ref. [232].

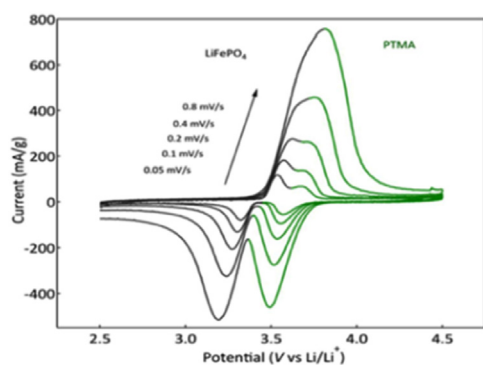


Fig. 16. Voltammograms recorded between 2.5 and 4.5 V vs. Li/Li<sup>+</sup> at different scan rates. Adapted from Ref. [233].

nanoflower hybrid structure supercapacitors in KOH solution is shown in Fig. 15. The CV curves are attained at a scan rate of 10–100 mV/s<sup>−1</sup> at the potential window of 0.5–0.7 V [232]. The Co<sub>3</sub>O<sub>4</sub> nanowire/nanoflower hybrid structure display superior rate capability of 1000 mV/s<sup>−1</sup> due to quick ion transport on the electrode surface [232]. CV analysis of another hybrid electrode material composed of LiFePO<sub>4</sub> and poly (2,2,6,6-tetramethyl-1-piperinidyl-4-yl methacrylate) (PTMA) [233] is shown in Fig. 16. From the CV plot, two distinct peaks are observed at low scan rates while only one peak can be seen during higher scan rates [233]. The peak current intensity and scan rates are important in the determination of electrodes redox kinetics.

#### 5.2.1. Material requirement

The capacitive assessment of a material is achieved by application of CV. For supercapacitor behavior, the material should inherit the electrochemical assets analogous to an electrical property of a normal capacitor. For instance, CV of conventional capacitor yields rectangular plot because capacitance is not linked directly with potential with the existence of mirror image around zero current line [230]. The capacitance varies between two vertical current switches at potential extremes i.e. current alters its sign when the path of the potential sweep is altered. This means that when different potential sweep rates guide the charging of a capacitor, the CV current becomes directly proportional to potential sweep rate. These form the three basic conditions for a material to show capacitance which is summed up as;

1. The existence of mirror image around zero current line,
2. The existence of vertical current switches at potential extremes, and
3. Direct correspondence of current with potential sweep rate.

These three conditions are mandatory for a material to exhibit capacitance. EDLC composed of carbon material satisfies all three conditions. Pseudocapacitor also satisfies all the three conditions but CV plot is not necessarily rectangular owing to the dependence of capacitance on potential [231].

#### 5.2.2. Steady potential window determination

The steady potential window of a supercapacitor is obtained by CV analysis. The determination involves analysis of CV plot in the potential range likely for a supercapacitor device. The assessment of steady potential window is determined by the transformations of CV shape and size depending upon the material under investigation. The size transformation may be as a result of dissolving of the electrode material or detachment of electrical contact with the surface through repeating cycles of polymers [234].

#### 5.3. Energy and power density assessment

This assessment leads to the evaluation of overall performance of a

supercapacitor for which Ragone plot is used. Ragone plot gives the overall electrochemical profile of the supercapacitor device in contrary to the single electrode [235]. However, numerical calculation of energy density is obtained by integrating the discharging curves proceeding to the equation:

$$E = \int_{V_1}^{V_2} C(V_1 + V_2)(V_2 - V_1) \quad (12)$$

where  $E$  stands for the energy density (Wh kg<sup>−1</sup>),  $C$  denotes capacitance (F g<sup>−1</sup>).  $V_1$  and  $V_2$  represent the charge and discharge voltages respectively.  $(V_2 - V_1)$  denotes the specific voltage window symbolizing capacitive behavior of the device.

Now if any of the voltage components is equal to zero, the energy density becomes dependent on the present component only [235], i.e.

If  $V_1 = 0$ ,

$$E = \frac{1}{2} CV_2^2 \quad (13)$$

Eq. (12) represents the case of EDLC with  $V_1 = 0$  (minimum) is ideal for its capacitive requirement. But for hybrid supercapacitor,  $V_1$  must be higher than zero. Hence, Eq. (13) gives the energy density of a hybrid supercapacitor.

The correlation between energy and power densities is given by the equation:

$$P = \frac{E}{t} \quad (14)$$

where  $P$  symbolizes power density (W kg<sup>−1</sup>),  $E$  denotes energy density (Wh kg<sup>−1</sup>) and  $t$  is time. Maximum power density ( $P_{\max}$ ) is dependent on the square of the maximum voltage ( $V_{\max}$ ) and equivalent series resistance denoted by  $R_s$  as shown in the equation below.

$$P_{\max} = \frac{V_{\max}^2}{4R_s} \quad (15)$$

The ESR is the overall sum of resistances corresponding to electrode, electrolyte and the diffusion resistances respectively of ions in electrode pores [105]. Apart from the numerical parameters both energy as well as power densities explicitly are reliant on mass loading of active material. There exists an inverse dependency of energy and power density on mass loading and according to Gogotsi et al. [234] the low mass loading and relatively low current always yield enhanced electrochemical performance.

#### 5.4. Electrochemical impedance spectroscopy (EIS)

Electrochemical impedance spectroscopy (EIS) measurements give the impedance of a supercapacitor at a specified potential. The voltage amplitude range for such measurements is low ranging from 5 mV to 10 mV corresponding to the wide frequency limits ranging from 0.01 Hz to 100 kHz [105]. These consequences are obtained by a specific plot (called as Nyquist plot) as shown in Fig. 17 for asymmetric supercapacitor. The Nyquist plot displays the impedance spectra over known frequency ranges [232].

The Nyquist plot comprises three regions [236]. The region of higher frequency (greater than 10<sup>4</sup> Hz) marking a semicircle in the plot produced is due to the interfacial resistance. The second region of high to medium frequency (10<sup>4</sup>–10<sup>1</sup> Hz) marking a vertical line on the plot owing to the resistance of charge transfer. The third region of least frequency (less than 1 Hz) presenting an imaginary line along the vertical line of the second region representing the capacitive behavior [236]. From this imaginary portion of impedance ( $Z$ ) related to frequency can be calculated using EIS measurements. The equation governing capacitance is:

$$C = \frac{1}{2\pi f|Z|} \quad (16)$$

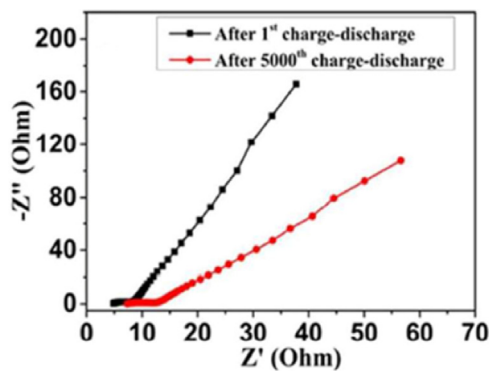


Fig. 17. Typical Nyquist plot of fabricated symmetric  $\text{Co}_3\text{O}_4$  based symmetric supercapacitor. Adapted from Ref. [232].

where  $C$  represents capacitance,  $f$  represents frequency and  $Z$  represents impedance. This equation calculates the capacitance of a linear portion of  $\log |Z|$  versus  $\log f$  termed as Bode plot. From Bode plot inverse relation between capacitance and frequency can be displayed [236].

### 5.5. Assessment of cell reliability

Reliability is defined as the probability of a device to perform the intended functions in accordance with stated or specified condition related parameters at the specified time duration [237]. Reliability yields result feasible of a large group of materials under similar treatment. Reliability of a material is reliant on the material design, its usage and the environment where it has to be used along with material quality [105]. The cell reliability assessment yields the aging of capacitors in general. The faster aging of casted electrochemical capacitors operated at a fixed potential and numerous temperatures were described by Kobayashi yielding Weibull life cycle models [237]. An efficient approach to congregate the electrochemical cell reliability information in a voltage and temperature range regarding commercial electrochemical capacitors was proposed by Galiński et al. [238]. The cell reliability forms an important tool concerned before employing a supercapacitor assembly such that it can perform according to the needs. This measurement involves the study of an electrochemical capacitor from its functional start till it stops working. This assessment is in regards to individual component examining to accurately determine its respective reliability and lifetime especially till the end of life. For the passive components in the cell, the reliability assessment is done in a well-prescribed laboratory in terms of field data [237].

Numerous approaches have been put forward so far for reliability assessment. The most general approach is based on the assessment of similar supercapacitor cells at diverse stress stages [238]. This determines each cell entity's response to the applied stress over time. The lifetime of the component is determined at its death and accordingly, the data can be used to predict the lifetime of similar supercapacitor components. An arrangement of cells is tested for aging or lifetime at elevated stress levels and faster testing rate compared to what they are normally accustomed to [237].

The aim of this assessment at faster or accelerated testing is to enhance the fatal rate to get the lifetime data in a shorter duration of time. The reliability assessment restrained to more groups for testing yields better statistics and defines the lifetime more precisely [237]. However, this entails extended test duration, more effort at elevated expenditure. Therefore, a stability factor is essentially concerned to the size of the testing group and expenditure. By application of standard statistical models, the correspondence among the size of the test group and lifetime models can be created. The electrochemical supercapacitor death may be defined by the whole loss of functionality leading to a dead short circuit. There are also factors leading to the death of supercapacitor including electrolyte outflow or cell rupture or packing fault.

The supercapacitor death is taken at the point where it reaches an obvious and definite failure.

The parameters directly linked to performance are operating voltage, temperature and to some extent humidity. The approximation rule of temperature for electrochemical supercapacitor is  $10^\circ\text{C}$  implying that  $10^\circ\text{C}$  descent in temperature increase the lifetime of a cell by the factor of two. This approximation rule holds true for most of the electrochemical supercapacitors at their maximum operating voltage and temperature conditions [239]. The approximation rule for voltage, that is with 0.1 V decrease in voltage elevates the lifetime to twice the existing value. The voltage approximation rule is followed by symmetric electrochemical supercapacitor in a non-aqueous electrolyte. The operating voltage ( $V$ ) and temperature ( $T$ ) correspond to lifetime given by normalized equation as:

$$\frac{\tau(T, V)}{\tau(T_0, V_0)} = 2^{\left[\frac{T_0 - T}{10}\right]} \times 2^{\left[\frac{V_0 - V}{10}\right]} \quad (17)$$

where  $\tau(T_0, V_0)$  corresponds to the characteristic lifetime at  $T_0$  and  $V_0$  (initial values) testing state also termed as endurance state. Lifetime allocation of a specific supercapacitor at all normal operating conditions comprises of similar Weibull shape factor. The low-stress characteristics show extended life while the high-stress characteristics correspond to reduced lifetime, however, the shape remains unaltered. However, in case of operation at extreme stress situations the shape changes based on addition or number of failure modes [238].

Another efficient approach regarding measurement of reliability is concerned with simultaneous lifetime determination of various cells at different specified voltage and temperature conditions. The intention is pointed towards extending the range of application and appropriately assorted for statistical balance. The data obtained from the groups is taken jointly for general model creation covering all temperature and voltage situations. This general model is essential in furnishing performance and future lifetime predictions.

## 6. Design and fabrication

The designing of a supercapacitor is concerned with the alignment of individual components in an overall configuration [210]. Hybrid supercapacitor consists of binary electrode sections comprising of either same material or different materials but of same dimensions along with microporous separator all inserted in an electrolyte. The entire system is squeezed between current collectors acting as terminals while charging and discharging [220]. The electrodes are usually of thickness nearly equivalent to  $100\ \mu\text{m}$  for systems in the non-aqueous electrolyte, whereas slightly thicker for an aqueous electrolyte. Separators are usually of  $24\ \mu\text{m}$  thickness whereas current collectors are of  $50\ \mu\text{m}$  thickness [105]. This description constitutes a bipolar design. The most common design related to supercapacitors is the cell design consisting of organic electrolyte. The entire components of supercapacitor are portrayed in a single cell. The combination of such singular cells together can deliver better performance regarding DC applications [239]. The aim regarding the combination of such singular cell components owes to high reliability than the cell combination in a battery. The advantage of cell design is an accurate evaluation of parameters at any given moment. In addition to cell design, the asymmetric design is also holding its significance concerned to supercapacitor design mainly for hybrid supercapacitors. The asymmetric design consists of two different electrodes (EDLC and Faradaic) performing accordingly. This design significantly enhances the energy density of an electrochemical capacitor along with the reduction of self-discharge rate [210].

The designs for supercapacitor cells are coin cell design, cylindrical cell design and pouch type cell designing as shown schematically in Fig. 18(a–c). A coin cell design of  $\text{SiO}_2\text{-PPy}$  composite as shown in Fig. 18(a) contains the assembly of two electrodes along with the separator in a metallic case with the addition of an insulating polymer



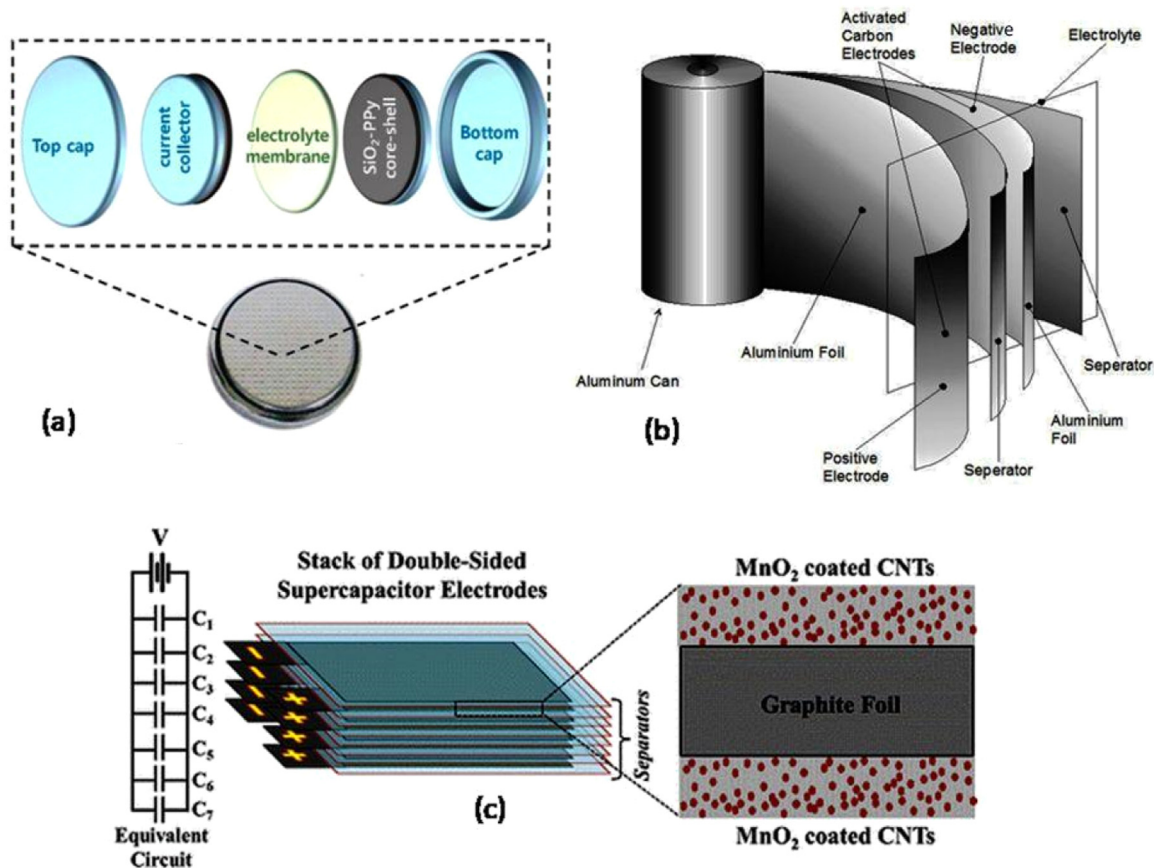


Fig. 18. Schematic representation of Supercapacitor design; (a) coin cell type design. Adapted from Ref. [239], (b) cylindrical cell design. Adapted from Ref. [241] and (c) pouch type cell design. Reproduced with permission from Ref. [240].

like Teflon [239]. The metallic case is conductive and the insulating polymer is only added to avoid electrolyte leakage and short circuit. The entire assembly is sealed by the application of suitable pressure to the metallic casing [240]. The requirements for such design are:

- Thin electrodes.
- Low active material concentration.

These form the limiting case for such design as well. The cylindrical cell design is the most broadly preferred and used design for supercapacitor with a heavy mass of active material loading [60]. The schematic illustration of a cylindrical design is shown in Fig. 18(b). First, the electrodes are drawn in the form of long rectangular sheets which are later on rolled to fit into cylindrical metal casing along with same dimensional separators. The connections between the current collector and the rolled sheets of electrodes are soldered [241]. The pouring of electrolyte solution into the casing is done after completion of the electrode-separator assembly. Then finally sealing of the entire cell takes place with safety vents installation for safety in case of pressure accumulation.

The pouch type design as in the case of MnO<sub>2</sub> coated on CNT involves layer by layer stacking of the electrode-separator-electrode and so on as shown in Fig. 18(c). This design is crucial for multiple electrode pile arrangement. The multiple electrodes are first soldered with their individual current collectors and later on the connection of desired current collectors is made accordingly. Instead of metallic casings, the pouch design uses the polymer bag adding flexibility to the assembly. Apart from these, there is a minimum requirement of the components in the cell resulting in lower equivalent series resistance and brilliant performance [241].

The pro design process for supercapacitors involves component

fabrication. The component fabrication involves electrode fabrication and electrolyte preparation techniques by various means [239]. The requirement for electrode preparation is homogenized paste or slurry formation of active materials with a binding agent in a solvent [240]. This paste or slurry can either be pressed on a plate by means of hot pressing followed by drying or by more solvent dilution of the paste or slurry and spraying like paint on the current collector [239]. The common fabrication technique is printing in which the fabrication substrate is directly added to the surface of the electrode by means of spraying paint or by the means of printing [241], by templates or ink-jet printing [242] and casting methods [240] etc. The outcome of the printing method is greater surface coverage and deposition on non-conventional surfaces including, paper, polymers and flexible sheets. The spray of printable material is followed by solvent evaporation. Like a printed carbon nanotube network with a fabricated film (ink-jet printing). On the other hand, by spraying technique dual functionality materials can be formed that can function as an electrode as well as charge collectors like in case of single-walled carbon nanotubes (SWCNTs) on the plastic substrate [241].

Likewise, ink-jet printing for fabrication of mono walls of CNTs on cloth and elastic surfaces for thin film electrode configuration is also widely used fabrication method [103]. This process uses an off the shelf ink-jet printer aiding to a controlled thickness, adjustable electrical properties along with preservation of the geometry. By using a similar process, nanowire electrodes of ruthenium oxide/SWCNTs were also fabricated [242]. The other fabricating method involves collateral lettering or portrayal with aid of graphite bar or pencil on cellulose paper [53]. The benefit of this technique is its non-requirement of solvent with the limitation of practical feasibility during batch processing. The preparation of electrolyte which is only reliant on the nature of electrolyte is easy as compared to that of electrode preparation. For



instance, the organic electrolytes are prepared inside a moisture free environment.

The material design for hybrid supercapacitor holds a key position while manufacturing. For instance, the design process involved in the synthesis of the hybrid assembly of  $\text{Li}_4\text{Ti}_5\text{O}_{12}$  and activated carbon is termed as ultra-centrifuging force (UCF) method [61,243]. The nanostructure is composed of nanocrystalline composites of  $\text{Li}_4\text{Ti}_5\text{O}_{12}$  particles dissipated on activated carbon [244]. The hybrid structure synthesized by UCF method possessed higher conductivity [245]. The composite material acts as a negative electrode while the activated carbon acts as a positive electrode in the creation of nano-hybrid capacitor furnishing elevated power and energy density.

## 7. Current perspectives and challenges

The hybrid supercapacitors are currently available commercially and their ability to combine higher energy density along with long-term stability marks their presence as appropriate devices for applications requiring unconstrained energy for their smooth operation like in hybrid electric vehicles. Their usage suffers limitations due to limited power proficiency. The consideration of nanostructured materials has already provided a better tool endorsing the power proficiency in the faradaic electrodes. The microstructural variations prevailing on cycling negotiates the effect of nanostructure consideration reliant on the electrolyte. The power capability improvement is attained considering the aqueous asymmetric electrochemical supercapacitor. This type of hybrid supercapacitor entails the use of both EDLC and pseudocapacitive electrodes. Currently, the core-shell designing of such perspective is under the limelight, but so far there is no such commercially available system. The usage of aqueous electrolyte offers a key benefit of developing low-cost materials. The main highlighting direction towards the hybrid supercapacitors is to produce a new generation of hybrid materials with splayed cell voltage coupled with electrode capacitance along with eco-friendly nature and cheap cost. The hybrid or asymmetric capacitors possess an inherent benefit of safe operation, least impact on the environment due to electrolyte vapors in case of cell eruption. However, the optimization of cell components comprising of the formulation of electrolyte which can be ideal for low-temperature operation in addition to resistance to oxidation offered by current collectors in an aqueous medium. There exist a large number of hybrid supercapacitors, EDLC's, pseudocapacitors, lithium-ion hybrid capacitors etc. For the high voltage requirements, supercapacitors are assembled in series inside a bank of cells yielding colossal supercapacitors units. This approach finds application in few sectors while facing the drawbacks in applications due to critical power source size. The problems could be altered by designing the whole unit of supercapacitors in an array of separated electrochemical cells with same plane fabrication. Such a configuration provides control over the current and voltage output.

The nanomaterials incorporated with various forms of carbon have been synthesized by many strategies ranging from hydrothermal treatment to simple heat treatment of carbon with nitrogen-containing complexes causing carbonization of nitrogenous complexes under an inert atmosphere. The heat treatment procedures due to the presence of nitrogen, however, reduce the surface area and conversely, approach to increase the surface area results in a decrease in nitrogen content mostly. Clearly, there is still an urgent need for further innovations related to synthesis of hybrid supercapacitors, so that the parameters required for better-performing systems. The challenges regarding the synthesis of such hybrid systems are:

- Development of an effective method which enables precision over control and yields ordered porous structures.
- Controlling the behavior of nitrogen to achieve better and tunable electrochemical properties.
- Further improvement in the development of cost-efficient and

scalable preparation methods.

The key issues in the development of supercapacitors are discussed in this section.

### 7.1. Material properties and thickness of electrodes

The materials explored for supercapacitor properties must inherit the properties like high surface area, pore size distribution etc. The materials especially carbonaceous materials exhibit properties like a large fraction of micropore resulting from small pores, permits free in and out-diffusion of electrolyte ions. As such only a little fraction of surface area is utilized for EDLC and a significant fraction causes pore resistance which adds to the total resistance of the electrode material. Therefore, it requires the development of materials with pore size distribution for a specific application.

The thickness of an electrode also plays a vital role in the performance of a supercapacitor. For a particular application like hybrid vehicles, the electrodes thickness should be of the order of less than  $150\text{ }\mu\text{m}$  and the large fraction of micropores should be of diameter  $10\text{--}20\text{ }\text{\AA}$ . Therefore, it is essential to consider the thickness of the electrode in relevance to its applicability.

### 7.2. The contact resistance between material particles and electronic resistivity

The supercapacitor electrodes must display electronic resistance less than  $1\text{ m}\Omega\text{-cm}$ , in order to get low resistance values for the cell. Therefore, to ensure better performance, the contact resistance between the materials forming the electrode must also be low. The use of conducting binder or any process capable of connecting the elements atomically like sintering can prove beneficial. It is essential that the combination of the active electrode material with a binder or atomically connecting the elements should not impart any changes to the supercapacitive properties of the active material. The requirement of reducing resistivity is still a problem in the development of many supercapacitors.

The electronic resistivity of the supercapacitor is proportional to the resistivity of the electrolyte and size of ions. This statement holds its grounds only in case of organic electrolytes. The aqueous electrolytes show an electronic resistivity of lower than  $1\text{--}2\text{ }\Omega\text{ cm}$  while organic electrolytes show an electronic resistivity of  $20\text{--}60\text{ }\Omega\text{ cm}$ . In addition to that the pore size requirement for organic electrolytes is also greater ( $15\text{--}20\text{ }\text{\AA}$ ) than that of aqueous ones ( $5\text{--}10\text{ }\text{\AA}$ ). Therefore, while developing a supercapacitor apart from electrode material consideration, electrolytes should be given importance as well. The other key issues while developing a supercapacitor are;

- The bonding between the current collector and electrode material should yield low contact resistance. Therefore, it is important to have a high degree of adhesion between the current collector and electrode material,
- Uniformity in configuration and stacking of the cells in the supercapacitor ensures quality control and to avoid self-discharge.
- It is important to choose the material of high purity for both electrode and electrolyte materials as it impacts the current leakage and cycling life.

Considering all these aspects and to meet these, it is essential to develop such tools to ensure better performing supercapacitors.

## 8. Applications

The ever-improving performance of supercapacitor leads to constant increment in their applications. Last decade has seen the extensive dominance of rechargeable batteries in the energy storage business. The



Fig. 19. Trolley bus of Aowei Technology Co. Ltd. based on  $\text{Ni}(\text{OH})_2\text{-AC}$  Supercapacitor [254].

growth in demand for enhanced energy storage for diverse applications regarding electronic portability to hybrid electric vehicles is rapidly increasing. The need in the sector of energy storage is performance optimization and cost reduction [240]. The supercapacitor applications are mentioned in the upcoming sections.

### 8.1. Public sector applications

The day to day applications include the products of easy operation. The freestyle (cordless) screwdriver propelling only via supercapacitors manufactured by Coleman Company Inc. which operates for less time compared to the one using a rechargeable battery. The limitation being the runtime which is half compared to the battery model, while the advantage of 90 s charging and charge retaining capability. However, according to Cameron [246], there is no risk of damaging the components while interruption of the charging cycle. Also, products like remote controls operating on supercapacitors have been developed by Maxwell Technologies (supercapacitor manufacturer) in collaboration with Celadon. The remote control was initially operated by use of two AAA batteries while operation on supercapacitor induced quick charging function [246]. According to Cresce et al. [247], the lifetime of supercapacitor surpasses the remote lifetime. In digital cameras, supercapacitors are used for producing flashes. Latest addition is the portable speakers developed by Sam Beck (Blueshift) in line with inbuilt supercapacitor assembly. The playback time is up to 6 h on full volume range after charging for 5 min according to Denison [248]. Prior to this, supercapacitors were basically used for memory backup and actuator applications [249]. They are used as stabilizers in wind energy and photovoltaic based power line systems and as such are used in renewable and sustainable energy sources. Hybrid supercapacitors supply short energy bursts to wind turbine due to instant response of supercapacitor to unpredictable weather changes [250]. The power cut situations are dealt by the presence of hybrid supercapacitors with a tendency to control blade orientation and providing protection for a wind turbine in extreme winds. Besides, the high number of cycles, energy compatibility with power density and lack of maintenance work in favor of hybrid supercapacitors.

In a security application, hybrid supercapacitors are used where the short duration of the power supply is necessary. The hybrid supercapacitor function in security systems is analogous to the function of the uninterrupted power supply (UPS) in computers. The Thames cable cars (Emirates Airline cable cars) are also comprised of hybrid supercapacitor energy systems facilitating the lights and air conditioning. The entire assembly is quickly charged yielding a ride time of 5 min [251]. The collaboration of solar energy along with supercapacitors as energy storage units to provide eco-friendly street lighting in Japan was done together by three Japanese companies Nippon-Chemi-Con in 2010

[249]. The assembly comprised of LED lamps along with solar boards to restrain solar energy through daytime, saved in supercapacitors (charging) while discharging of hybrid supercapacitors escorts lighting up the LED's during night time. Hence, providing clean energy system with higher sustainability and lifetime prior to the existing energy systems.

### 8.2. Automobiles and transport application

The well-known demand for automotive sector is the energy storage systems for multi-tasking operation like ignition, start-up, security, transmission and lighting etc. For instance, in the case of internal combustion engine, hybrid supercapacitor function can be linked to starting up the engine by providing instantaneous energy burst. Prior to that, the supercapacitor and the thermal motor in correspondence to their lifespan share compatibility. This property lowers the maintenance cost compared to the normal lead acid batteries or accumulators [252]. The electric vehicles or hybrid electric vehicles require high current during their charging for short duration of time producing a power pulsation which can be easily generated using a hybrid supercapacitor. The examples of such automobiles are the cars manufactured by Toyota and Mazda [253]. Toyota's Yaris Hybrid-R and PSA Peugeot Citroën use hybrid supercapacitors for power bursts, starting and stopping fuel saving arrangement allowing faster preliminary speeding up respectively [254].

Another important application in trend is hybrid supercapacitors in bigger electric vehicles like e-buses introduced by Aowei Technology Co., Ltd. (Shanghai, China) with quick charging property as shown in Fig. 19 [254]. The hybrid configuration of  $\text{Ni}(\text{OH})_2\text{-AC}$  is used in trolley bus with charging time of 90 s and distance range of 7.9 km attained at a maximum speed of  $44.8 \text{ km h}^{-1}$  and average speed of  $22 \text{ km h}^{-1}$  with the acceleration of  $0\text{--}40 \text{ km h}^{-1}$  in 16.5 s. In addition, the tramcar working on EDLC configuration with charging time of 30 s and distance range of 3–5 km has been developed by CSR Co. Ltd. (Chinese).

The application of supercapacitors in regenerative braking is already well-known. This is achieved by stopping the vehicle while trapping its braking energy. This was seen in a tram in Switzerland utilizing one-ton hybrid supercapacitors assembly installation to the tram. Similar sort of assembly was utilized on trams in Paris and Belgium consisting of the combination of 48 supercapacitors installed to each vehicle developed by Maxwell. The charging time being 20 s at each station, the trams successfully achieved stopping by means of regenerative braking [255]. By means of regenerative braking, there is a recovery of braking energy which requires devices with quick storage and high cycle rate. Therefore, hybrid supercapacitors are an ideal choice for such applications. By capturing the braking energy, the hybrid supercapacitors can provide this energy for ignition of the diesel engine and in speeding up. Up to 30% energy savings can be achieved by this recovery.

The effective consideration on the usage of a supercapacitor with public transportation was the motivating feature initially. The usage related to an operation in the transport means such as trucks and buses to improve energy efficient delivery in order to overcome the wastage of heat energy during a halt while the engine is running. The perspective of supercapacitors is to utilize this energy on conversion to electrical energy to propel acceleration assistance needs. This adds to eco-saving by limiting the emission of  $\text{CO}_2$  and consumption of fuel. The buses powered by supercapacitors entirely were developed by Sinautec company while recharging stations kept at the bus stops [256]. Also, the emergency door operation and eviction slide operation within Airbus 380 jumbo jet is accompanied by the application of hybrid supercapacitors [257]. The wider transport means utilizing hybrid supercapacitors in the railways and metro trains. For example the development of a prototype of two-car based light metro by CSR Zhuzhou Electric Locomotive Corporation of China in August 2012. The light metro contains hybrid supercapacitor unit mounted on the roof [258].



Fig. 20. Supercapacitors manufactured by Tecate group for different defence applications [261].

The Hong Kong's South Island metro lines [259], the metros developed by SYTRAL in Lyon [260], France etc. are some other examples of railway using hybrid supercapacitors for their operation.

### 8.3. Defence and military applications

The tools based on batteries like navigators, sensor, communication tools are an open field for hybrid supercapacitor applications. The radar system, electromagnetic pulse weapons, torpedoes etc. can also be operated using a suitable assembly of hybrid supercapacitor [261]. Tecate group has manufactured many supercapacitor systems for military applications as shown in Fig. 20 [261]. The applications requiring high specific power are phased array radar antenna, avionics display gadgets, airbag exploitation power, GPS and missiles.

### 8.4. Computers and memory backup chips

Memory backup is one of the most prominent functions of hybrid supercapacitors in electronic devices pertaining to CMOS or micro-processor containing semiconductor memory devices [262]. Hybrid supercapacitor in such cases does not serve as an energy storage medium instead provides memory backup function during short power interruptions. Hybrid supercapacitors find their applications corresponding to the requirement of fluctuating loads like laptops, portable media players etc. as a stabilizer of the power supply. They provide backup power for the shutdown of low power components like RAM, SRAM, PC cards and in UPS. The ability lies in the production of high pulse power for a short duration of time. The application of hybrid supercapacitor protects memory against any substantial potential drop regarding the primary power source. Hybrid supercapacitor assembly provides better results compared to the existing technology concerned with the UPS devices [263].

Hybrid supercapacitors also serve as a backup power supply in solid state drives (SSD's) intended to cache memory. The presence of hybrid supercapacitor highly supports the SSD during cache cleansing and gracefully shuts down during power failures without incorporating any loss of data [264]. A hybrid supercapacitor consisting of two-cell series

designed by linear technology is dedicated to backup functionality [265]. This system comprises of hybrid supercapacitor charger acting as charge pump with the adjustable output voltage and automated cell voltage balancing. In addition to these, low dropout regulator and a comparator dedicated to power failure acting as a switch amid normal and backup modes are also present in such backup systems. There are three voltage points regarding such backup systems [266];

1. When comparator suffers power failure the voltage point is termed as high trigger point (3.6 V).
2. Second voltage point termed as standby mode point (3.15 V) and
3. When the power is held up by the system in absence of battery power termed as backup mode point (3.10 V).

### 8.5. Medical and industrial applications

In the medical world, the hybrid supercapacitors can be related to high voltage pulse delivery applications. As such they are fed to defibrillators delivering 500 J thrust of energy to jolt the heart to its normal functioning [265]. The patients suffering from mental trauma are dealt with a similar sort of procedures. The ventilator backup can be a new application of hybrid supercapacitors along with dental science etc. Related to backup power source JSR Micro constructed a hybrid supercapacitor for medical imaging equipment [266].

This is the widest sector for hybrid supercapacitor applications, starting from industrial electronics like automated meter reading (AMR) to the emergency backup power source to avoid any disastrous breakdown until power restoration. The stability factor of supercapacitors led to the development of supercapacitor-powered drills by FastCAP [267]. These drills are employed to emulate petroleum and geothermal energy sections. The drills have an advantage of functionality at high temperatures without escorting the overcharge. The drills developed by Dewalt Power Tool Company use supercapacitors for their functioning (Fig. 21) [268].

In addition to that, there are applications regarding the collaboration of batteries and hybrid supercapacitors in the industrial sector. The collaboration restrains energy benefits from both energy storing device





Fig. 21. Power drill developed by Dewalt using supercapacitors [268].

technologies and could prove beneficial in many power-related applications.

#### 8.6. In electricity grids, power quality and battery monitoring

The electricity grids deploy hybrid supercapacitors for enhancing reliability. This is achieved by adding energy storage means. The stored energy can be utilized in cases of modest power generation or no power generation. The report published by US Department of Energy (DOE) in February 2010 recognized over 20 applications for this stored energy [269]. The storage systems provided energy for the duration in the range of seconds to hours. The storage duration of about 12 h is done during excess generation corresponding to low demand and used when demand is high. Utilization of hybrid supercapacitors for such grid reduces storage cost per unit of energy as compared to batteries or other types of equipment. Hybrid supercapacitors assembly can provide an alternative for bulk energy storage. Predominantly asymmetric design inserted in aqueous electrolytes [270]. Asymmetric supercapacitors possess the advantage of designing in accordance with the requirements. The number of cycles required for the bulk storage is about 5000 cycles. The two asymmetric systems prescribed for such application are activated carbon/lead oxide with  $\text{H}_2\text{SO}_4$  as electrolyte having an operational voltage of 2 V and specific energy of nearly  $19 \text{ W kg}^{-1}$  while, the other comprises of EDLC-Sodium intercalated electrodes with a neutral aqueous electrolyte [271]. These asymmetric systems possess the ability to present desired storage and cycle life.

The hybrid supercapacitors can be used as an alternative energy storage device in order to improve the reliability and power distribution quality. Static synchronous compensator supercapacitor system is developed to absorb and inject power from distribution line in order to regulate a constant voltage during voltage fluctuations. However, such systems require a DC energy device from which energy can be drawn or stored. In some systems, the battery performance is reduced due to current profiles of short and high current bursts. To improve battery performance, a supercapacitor can be combined with the battery. The presence of supercapacitor will ensure smooth functioning of the battery by relieving it from high load demands at peak power requirements. The supercapacitor reduces the pulsed current which is drawn from the battery thereby extending the battery life.

#### 8.7. Future applications and scope

For any particular electrode material, it exhibits strong points and

limitations. The higher energy density and higher cycle life are accomplished by employing two different electrodes in hybrid electrochemical supercapacitor [272,273]. To furnish the desired advantages of different electrode materials the proposal of hybrid nanocomposite supercapacitor has been put forward by many researchers. There exist numerous materials from which nanocomposite hybrid supercapacitors can be prepared. Similar sort of choices of materials exists for EDLC and pseudocapacitor electrodes. The integrating systems comprising of batteries and supercapacitors termed as hybrid devices with one shadowing the limitation of the other. Battery electrode contributes to the energy storage advantage while the supercapacitor electrode contributes to the power density advantage. This results in the formation of a system with enhanced power and energy densities. The sector for such collaboration can be the hybrid vehicles. The urge to produce slim and brittle electronic devices such as transistor and others in the making requires a consummation of energy source. Currently, the successful development of such integrated devices has already been achieved [257]. The development of lightweight components by Volvo composed of carbon fibers and polymer resins acting as a supercapacitor has been used in electronic vehicles. The lightweight supercapacitor has an advantage of lesser weight and easy molding into the desired shape compared to the batteries. The Volvo prototype S80 comprises of supercapacitor using brake energy [274]. The concept of double hybridization opens new doors for supercapacitor applications with the combination of nanohybrid electrode and activated carbon capacitive electrode [275]. In the last decade, great progress has been made in the development of supercapacitors. The current progress is towards the development of cost-effective, portable and sustainable supercapacitor devices by means of different synthesis methods to enhance their energy storing capacity. With environment cautiousness and increasing fuel pricing, the supercapacitors can prove more exciting in becoming ideal energy sources in the future.

## 9. Conclusions

This review article elaborates the current status and the advancement in the field of supercapacitor and provides an insight into the need for supercapacitors in the modern world. The principles and mechanism of storage along with the classification of supercapacitors have been reported. The need for hybrid supercapacitors can be justified due to the limitations of current energy storage devices. It is clear that each type of supercapacitors like EDLC and pseudocapacitor find their applications as per their tendency. This factor limits their broader usage and as such, it is essential to develop hybrid supercapacitor systems to increase the applicability range. The applications of the hybrid supercapacitors are on the rise especially in the field of hybrid energy vehicles. As such, it is important to develop new supercapacitor materials with various techniques to maximize their usage. Supercapacitors can prove more feasible and sustainable energy storing devices than its contemporaries when synthesized by optimized methods and fabricated through proper means to avoid losses due to resistance and current leakage. The field for research pertaining to supercapacitors is wide open for exploration and development of new advanced materials for such applications has great potential in the future.

## References

- [1] Kim BK, Sy S, Yu A, Zhang J. Handbook of clean energy systems. John Wiley & Sons, Ltd.; 2014. p. 1–25.
- [2] Conway BE. Electrochemical supercapacitors: scientific fundamentals and technological applications. New York: Springer Science & Business Media; 2013.
- [3] Chan CK, Peng H, Liu G, McIlwrath K, Zhang XF, Huggins RA, et al. Nat Nanotechnol 2008;3:31–5.
- [4] Liu N, Huo K, McDowell MT, Zhao J, Cui Y. Sci Rep 2013;3:1919.
- [5] Simon P, Gogotsi Y. Nat Mater 2008;7:845–54.
- [6] El Brouji H, Briat O, Vinassa JM, Henry H, Woïrgard E. Microelectron Reliab 2009;49:1391–7.
- [7] Buïel E. Development of lead-carbon hybrid battery/supercapacitors. Proc Adv



- Capacit World Summit 2006;2006:17–9.
- [8] Gómez-Romero P, Ayyad O, Suárez-Guevara J, Muñoz-Rojas D. *J Solid State Electrochem* 2010;14:1939–45.
- [9] Lu Z, Chang Z, Zhu W, Sun X. *Chem Commun* 2011;47:9651–3.
- [10] Xie J, Sun X, Zhang N, Xu K, Zhou M, Xie Y. *Nano Energy* 2013;2:65–74.
- [11] Stoller MD, Park S, Zhu Y, An J, Ruoff RS. Graphene-based ultracapacitors. *Nano Lett* 2008;8:3498–502.
- [12] Wang G, Zhang L, Zhang J. *Chem Soc Rev* 2012;41:797–828.
- [13] Wang X, Yang YL, Fan R, Wang Y, Jiang ZH. *J Alloy Compd* 2010;504:32–6.
- [14] Chen PC, Shen G, Shi Y, Chen H, Zhou C. *ACS Nano* 2010;4:4403–11.
- [15] Lee SW, Kim J, Chen S, Hammond PT, Shao-Horn Y. *ACS Nano* 2010;4:3889–96.
- [16] Zhang D, Yan H, Lu Y, Qiu K, Wang C, Tang C, et al. *Nanoscale Res Lett* 2014;9:139.
- [17] Wang HW, Hu ZA, Chang YQ, Chen YL, Wu HY, Zhang ZY, et al. *J Mater Chem* 2011;21:10504–11.
- [18] Pandolfo AG, Hollenkamp AF. *J Power Sources* 2006;157:11–27.
- [19] Plitz I, DuPasquier A, Badway F, Gural J, Pereira N, Gmitter A, et al. *Appl Phys A: Mater Sci Process* 2006;82:615–26.
- [20] Li Y, Hasin P, Wu Y. *Adv Mater* 2010;22:1926–9.
- [21] Chai H, Chen X, Jia D, Zhou W. *Rare Met* 2011;30:85–9.
- [22] Naoi K. *Fuel Cells* 2010;105:825–33.
- [23] Huang S, Wen Z, Zhu X, Gu Z. *Electrochem Commun* 2004;6:1093–7.
- [24] Luo L, Wu J, Xu J, Dravid VP. *NUANCE Center. Microsc Microanal* 2014;20:1618–9.
- [25] Tachibana M, Ohishi T, Tsukada Y, Kitajima A, Yamagishi H, Murakami M. *Electrochemistry* 2011;79:882–6.
- [26] Yan J, Fan Z, Sun W, Ning G, Wei T, Zhang Q, et al. *Adv Func Mater* 2012;22:2632–41.
- [27] Gupta V, Gupta S, Miura N. *J Power Sources* 2008;175:680–5.
- [28] Fan Z, Yan J, Wei T, Zhi L, Ning G, Li T, et al. *Adv Funct Mater* 2011;21:2366–75.
- [29] Jorio A, Saito R, Hafner JH, Lieber CM, Hunter D, McClure T, et al. *Phys Rev Lett* 2001;86:1118.
- [30] Inoue H, Morimoto T, Nohara S. *Electrochem Solid State Lett* 2007;10:A261–3.
- [31] Zhou WJ, Zhang J, Xue T, Zhao DD, Li HL. *J Mater Chem* 2008;18:905–10.
- [32] Pandolfo T, Ruiz V, Sivakkumar S, Nerkar J. *Supercapacitors: materials, systems, and applications*. 2013. p. 69–109.
- [33] Huang J, Sumpter BG, Meunier VA. *Chem- Eur J* 2008;14:6614–26.
- [34] Vivekchand SRC, Rout CS, Subrahmanyam KS, Govindaraj A, Rao CNR. *J Chem Sci* 2008;120:9–13.
- [35] Zhang LL, Zhao XS. *Chem Soc Rev* 2009;38:2520–31.
- [36] Huang J, Sumpter BG, Meunier V. *Angew Chem Int Ed* 2008;47:520–4.
- [37] Chmiola J, Yushin G, Gogotsi Y, Portet C, Simon P, Taberna PL. *Science* 2006;313:1760–3.
- [38] Guidi G, Undeland TM, Hori Y. *IEEE Trans Ind Appl* 2008;128:418–23.
- [39] Barrade P, Pittet S, Rufer A. *PCIM2000 Power Conversion and Intelligent Motion, Nürnberg, Germany; 2000*.
- [40] Petreus D, Moga D, Galatus R, Munteanu RA. *Adv Electr Comput Eng* 2008;8:15–22.
- [41] Kruusma J, Tõnisoo A, Pärna R, Nõmmiste E, Tallo I, Romann T, et al. *Electrochim Acta* 2016;206:419–26.
- [42] Ania CO, Pernak J, Stefaniak F, Raymundo-Piñero E, Béguin F. *Carbon* 2009;47:3158–66.
- [43] Gauchia L, Bouscayrol A, Sanz J, Trigui R, Barrade P. In: *Proceedings of the vehicle power and propulsion conference VPPC. IEEE; 2011*, p. 1–62011.
- [44] Burke AR. *Electrochim Acta* 2007;53:1083–91.
- [45] Helmholtz HV. *Ann der Phys* 1879;165:211–33.
- [46] Endo M, Takeda T, Kim YJ, Koshiba K, Ishii K. *Carbon Lett* 2001;1:117–28.
- [47] Gouy MJ. *Phys Theor Appl* 1910;9:457–68.
- [48] Xu MW, Bao SJ, Li HL. *J Solid State Electrochem* 2007;11:372–7.
- [49] Chapman D. *Lond Edin Dub Philos Mag J Sci* 1913;25:475–81.
- [50] Stern O. *Z Elektrochem* 1924;30:1014–20.
- [51] Chen X, Paul R, Dai L. *Natl Sci Rev* 2017;4:453–89.
- [52] Chavhan MP, Ganguly S. *Ionics* 2017;23:2037–44.
- [53] Seyedsalehi M, Goodarzi M, Barzanouni H. *J Biodivers Environ Sci* 2014;4:102–11.
- [54] Gomibuchi E, Ichikawa T, Kimura K, Isobe S, Nabeta K, Fujii H. *Carbon* 2006;44:983–8.
- [55] Zhao Y, Zheng MB, Cao JM, Ke XF, Liu JS, Chen YP, et al. *Mater Lett* 2008;62:548–51.
- [56] Xu B, Wu F, Chen S, Zhang C, Cao G, Yang Y. *Electrochim Acta* 2007;52:4595–8.
- [57] Balducci A, Bardi U, Caporali S, Mastragostino M, Soavi F. *Electrochem Commun* 2004;6:566–70.
- [58] Fang Y, Liu J, Yu DJ, Wicksted JP, Kalkan K, Topal CO, et al. *J Power Sources* 2010;195:674–9.
- [59] Banerjee S, Sharma YC. *J Ind Eng Chem* 2013;19:1099–105.
- [60] Boehm HP. *Carbon* 2002;40:145–9.
- [61] Frackowiak E, Béguin F. *Carbon* 2001;39:937–50.
- [62] Cottineau T, Toupin M, Delahaye T, Brousse T, Belanger D. *Appl Phys A* 2006;82:599–606.
- [63] Hu CC, Chang KH, Lin MC, Wu YT. *Nano Lett* 2006;6:2690–5.
- [64] Choi D, Blomgren GE, Kumta PN. *Adv Mater* 2006;18:1178–82.
- [65] Zhang H, Cao G, Wang Z, Yang Y, Shi Z, Gu Z. *Nano Lett* 2008;8:2664–8.
- [66] Fan LZ, Hu YS, Maier J, Adelhelm P, Smarsly B, Antonietti M. *Adv Func Mater* 2007;17:3083–7.
- [67] Frackowiak E, Lot G, Machnikowski J, Vix-Guterl C, Béguin F. *Electrochim Acta* 2006;51:2209–14.
- [68] Lota G, Grzyb B, Machnikowska H, Machnikowski J, Frackowiak E. *Chem Phys Lett* 2005;404:53–8.
- [69] Lee YH, Lee YF, Chang KH, Hu CC. *Electrochem Comm* 2011;13:50–3.
- [70] Qin C, Lu X, Yin G, Jin Z, Tan Q, Bai X. *Mater Chem Phys* 2011;126:453–8.
- [71] Jeong HM, Lee JW, Shin WH, Choi YJ, Shin HJ, Kang JK, et al. *Nano Lett* 2011;11:2472–7.
- [72] Hulicova D, Yamashita J, Soneda Y, Hatori H, Kodama M. *Chem Mater* 2005;17:1241–7.
- [73] Hulicova D, Kodama M, Hatori H. *Chem Mater* 2006;18:2318–26.
- [74] Hulicova D, Kodama M, Shiraishi S, Hatori H, Zhub ZH, Lu GQ. *Adv Func Mater* 2009;19:1800–9.
- [75] Lota G, Lota K, Frackowiak E. *Electrochem Commun* 2007;9:1828–32.
- [76] Jurewicz K, Frackowiak E, Béguin F. *Electrochem Solid State Lett* 2001;4:A27–9.
- [77] Frackowiak E, Jurewicz K, Szostak K, Delpeux S, Béguin F. *Fuel Process Technol* 2002;77:213–9.
- [78] Jurewicz K, Frackowiak E, Béguin F. *Appl Phys A Mater Sci Process* 2004;78:981–7.
- [79] Vix-Guterl C, Frackowiak E, Jurewicz K, Friebe M, Parmentier J, Béguin F. *Carbon* 2005;43:1293–302.
- [80] Béguin F, Friebe M, Jurewicz K, Vix-Guterl C, Dentzer J, Frackowiak E. *Carbon* 2006;44:2392–8.
- [81] Qu D. *Mechanism. J Power Sources* 2008;179:310–6.
- [82] Béguin F, Kierzek K, Friebe M, Jankowska A, Machnikowski J, Jurewicz K, et al. *Electrochim Acta* 2006;51:2161–7.
- [83] Bleda-Martínez MJ, Pérez JM, Linares-Solano A, Morallón E, Cazorla-Amorós D. *Carbon* 2008;46:1053–9.
- [84] Naoi K, Simon P. *J Electrochem Soc* 2008;17:34–7.
- [85] Demarconnay L, Raymundo-Pinero E, Béguin F. *J Power Sources* 2011;196:580–6.
- [86] Brousse T, Toupin M, Belanger D. *J Electrochem Soc* 2004;151:A614–22.
- [87] Ryu KS, Jeong SK, Joo J, Kim KM. *J Phys Chem B* 2007;111:731–9.
- [88] Khomenko V, Raymundo-Pinero E, Frackowiak E, Béguin F. *Appl Phys A Mater Sci Process* 2006;82:567–73.
- [89] Uvarov NF, Mateyshina YG, Ulihin AS, Yusin SI, Varentsova VI, Varentsov VK. *ECS Trans* 2010;25:11–6.
- [90] Toupin M, Brousse T, Bélanger D. *Chem Mater* 2002;14:3946–52.
- [91] Wu NL. *Mater Chem Phys* 2002;75:6–11.
- [92] Raymundo-Pinero E, Khomenko V, Frackowiak E, Béguin F. *J Electrochem Soc* 2005;152:A229–35.
- [93] Yang XH, Wang YG, Xiong HM, Xia YY. *Electrochim Acta* 2007;53:752–7.
- [94] Malak A, Fic K, Lota G, Vix-Guterl C, Frackowiak E. *J Solid State Electrochem* 2010;14:811–6.
- [95] Nam KW, Lee CW, Yang XQ, Cho BW, Yoon WS, Kim KB. *J Power Sources* 2009;188:323–31.
- [96] Fang B, Zhou H, Honma I. *J PhysChem B* 2006;110:4875–80.
- [97] Fang B, Kim M, Kim JH, Yu JS. *Langmuir* 2008;24:12068–72.
- [98] Babel K, Jurewicz K. *Carbon* 2008;46:1948–56.
- [99] Conway BE, Tilak BV. *Electrochim Acta* 2002;47:3571–94.
- [100] Lota G, Fic K, Frackowiak E. *Energy Environ Sci* 2011;4:1592–605.
- [101] Wu M, Gao J, Zhang S, Chen A. *J Porous Mater* 2006;13:407–12.
- [102] Zheng JP, Cygan PJ, Jow TR. *J Electrochem Soc* 1995;142:2699–703.
- [103] McKeown DA, Hagans PL, Carrette LP, Russell AE, Swider KE, Rolison DR. *J Phys Chem B* 1999;103:4825–32.
- [104] Lenardi C, Marino M, Barborini E, Piseri P, Milani P. *Eur Phys J B-Condens Matter Complex Syst* 2005;46:441–7.
- [105] Wang Y, Song Y, Xia Y. *Chem Soc Rev* 2016;45:5925–50.
- [106] Roldán S, Blanco C, Granda M, Menéndez R, Santamaría R. *Ang Chem Int Ed* 2011;50:1699–701.
- [107] Sathyaamoorthi S, Kanagaraj M, Kathiresan M, Suryanarayanan V, Velayutham D. *J Mater Chem A* 2016;4(12):4562–9.
- [108] Roldán S, Granda M, Menéndez R, Santamaría R, Blanco C. *J Phys Chem C* 2011;115:17606–11.
- [109] An KH, Jeon KK, Heo JK, Lim SC, Bae DJ, Lee YH. *J Electrochem Soc* 2002;149:A1058–62.
- [110] Lota G, Frackowiak E. *Electrochem Commun* 2009;11:87–90.
- [111] Taberna PL, Chevallier G, Simon P, Plée D, Aubert T. *Mater Res Bull* 2006;41:478–84.
- [112] Futaba DN, Hata K, Yamada T, Hiraoka T, Hayamizu Y, Kakudate Y, et al. *Nat Mater* 2006;5:987.
- [113] Reddy ALM, Shaijumon MM, Gowda SR, Ajayan PM. *J Phys Chem C* 2009;114:658–63.
- [114] Wang Q, Yong FN, Xiao ZH, Chen XY, Zhang ZJ. *J Electroanal Chem* 2016;770:62–72.
- [115] Duffy NW, Balds W, Pandolfo AG. *Electrochim Acta* 2008;54:535–9.
- [116] Machida K, Suematsu S, Ishimoto S, Tamamitsu K. *J Electrochem Soc* 2008;155:A970–4.
- [117] Wang Q, Nie YF, Chen XY, Xiao ZH, Zhang ZJ. *Electrochim Acta* 2016;200:247–58.
- [118] Naoi K, Nagano Y. *Supercapacitors: materials, systems, and applications*. 2013. p. 239–56.
- [119] Mastragostino M, Arbizzani C, Soavi F. *Solid State Ion* 2002;148:493–8.
- [120] Wang YG, Yu L, Xia YY. *J Electrochem Soc* 2006;153:A743–8.
- [121] Amatucci GG, Badway F, Du Pasquier A, Zheng T. *J Electrochem Soc* 2001;148:A930–9.
- [122] Yu H, Fan L, Wu J, Lin Y, Huang M, Lin J, et al. *RSC Adv* 2012;2:6736–40.
- [123] Rajkumar M, Hsu CT, Wu TH, Chen MG, Hu CC. *Mater Int* 2015;25:527–44.
- [124] Cericola D, Kötz R. *Electrochim Acta* 2012;72:1–17.
- [125] Khomenko V, Raymundo-Piñero E, Béguin F. *J Power Sources* 2008;177:643–51.
- [126] Park JH, Park OO, Shin KH, Jin CS, Kim JH. *Electrochem Solid State Lett*

- 2002;5:H7–10.
- [127] Burke A. Ultracapacitors: why, how, and where is the technology. *J Power Sources* 2000;91:37–50.
- [128] Cericola D, Novák P, Wokaun A, Kötter R. *J Power Sources* 2011;196:10305–13.
- [129] Sivakkumar SR, Pandolfo AG. *Electrochim Acta* 2012;65:280–7.
- [130] Cao WJ, Zheng JP. *J Power Sources* 2012;213:180–5.
- [131] Pickup PG. Modern aspects of electrochemistry. In: White RE, et al., editors. New York: Springer, Kluwer Academic/Plenum Publishers; 2002. p. 549–97.
- [132] Zhao S, Wu F, Yang L, Gao L, Burke AF. *Electrochim Commun* 2010;12:242–5.
- [133] Casalbore Miceli G, Gallazzi MC, Zecchin S, Camaioni N, Geri A, Bertarelli C. *Adv Funct Mater* 2003;13:307–12.
- [134] Schweiger HG, Obeidi O, Komesker O, Raschke A, Schiemann M, Zehner C, et al. *Sensors* 2010;10:5604–25.
- [135] Ansean D, González M, Viera JC, García VM, Alvarez JC, Blanco C. In: Proceedings of the vehicle power and propulsion conference (VPPC). IEEE; 2014. p. 1–6.
- [136] Marongiu A, Pavanariti T, Sauer DU. In: Proceedings of the electric vehicle symposium and exhibition (EVS27). World. IEEE; 2013. p. 1–11.
- [137] Huynh PL, Mohareb OA, Grimm M, Maurer HJ, Richter A, Reuss HC. In: Proceedings of the vehicle power and propulsion conference (VPPC). IEEE; 2014. p. 1–6.
- [138] Pastor-Fernandez C, Bruen T, Widanage WD, Gama-Valdez MA, Marco J. *J Power Sources* 2016;329:574–85.
- [139] Ma FX, Yu L, Xu CY, Lou XWD. *Energy Environ Sci* 2016;9:862–6.
- [140] Bai Y, Wang F, Wu F, Wu C, Bao LY. *Electrochim Acta* 2008;54:322–7.
- [141] Lin C, Ritter JA, Popov BN. *J Electrochem Soc* 1999;146:3639–43.
- [142] Ratchahat S, Kodama S, Sekiguchi H, Tanthapanichakoon W, Al-Ali K, Charinpanitkul TT, et al. *Eng J* 2015;19:95–104.
- [143] Zhu J, Jiang J, Sun Z, Luo J, Fan Z, Huang X, et al. *3D Small* 2014;10:2937–45.
- [144] Wang F, Zhan X, Cheng Z, Wang Z, Wang Q, Xu K, et al. *Small* 2015;11:749–55.
- [145] Celzard A, Collas F, Mareche JF, Furdin G, Rey I. *J Power Sources* 2002;108:153–62.
- [146] Laforgue A, Simon P, Fauvarque JF, Mastragostino M, Soavi F, Sarrau JF, et al. *J Electrochem Soc* 2003;150:A645–51.
- [147] Villers D, Jobin D, Soucy C, Cossement D, Chahine R, Breau L, et al. *J Electrochem Soc* 2003;150:A747–52.
- [148] Rakhii RB, Chen W, Hedhili MN, Cha D, Alshareef HN. *ACS Appl Mater Interfaces* 2014;6:4196–206.
- [149] Lee JE, Park SJ, Kwon OS, Shim HW, Jang J, Yoon H. *RSC Adv* 2014;4:37529–35.
- [150] Li L, Zhang Y, Shi F, Zhang Y, Zhang J, Gu C, et al. *ACS Appl Mater Interfaces* 2014;6:18040–7.
- [151] Zhou Z, Zhu Y, Wu Z, Lu F, Jing M, Ji X. *RSC Adv* 2014;4:6927–32.
- [152] Lota G, Fic K, Frackowiak E. *Electrochim Commun* 2011;13:38–41.
- [153] Li H, Cheng L, Xia Y. *Electrochim Solid-State Lett* 2005;8:A433–6.
- [154] Du Pasquier A, Plitz I, Menocal S, Amatucci G. *J Power Sources* 2003;115:171–8.
- [155] Wang X, Zheng JP. *J Electrochem Soc* 2004;151:A1683–9.
- [156] Dubal DP, Ayyad O, Ruiz V, Gomez-Romero P. *Chem Soc Rev* 2015;44:1777–90.
- [157] Amatucci GG. U.S. Patent No. 6: 252,762. Washington, DC: U.S. Patent and Trademark Office; 2001.
- [158] Yoshino A, Tsubata T, Shimoyamada M, Satake H, Okano Y, Mori S, et al. *J Electrochem Soc* 2004;151:A2180–2.
- [159] Choi H, Yoon H. *Nanomaterials* 2015;5:906–36.
- [160] Naoi K, Ishimoto S, Miyamoto JI, Naoi W. *Energy Environ Sci* 2012;5:9363–73.
- [161] Li Z, Zhang L, Amirkhiz BS, Tan X, Xu Z, Wang H, et al. *Adv Energy Mater* 2012;2:431–7.
- [162] Lee J, Kim J, Hyeon T. *Adv Mater* 2006;18:2073–94.
- [163] Li L, Song H, Chen X. *Electrochim Acta* 2006;51:5715–20.
- [164] Wang Q, Yan J, Wang Y, Ning G, Fan Z, Wei T, et al. *Carbon* 2013;52:209–18.
- [165] Yang M, Cheng B, Song H, Chen X. *Electrochim Acta* 2010;55:7021–7.
- [166] Huang Y, Liang J, Chen Y. *Small* 2012;8:1805–34.
- [167] Fan Z, Yan J, Zhi L, Zhang Q, Wei T, Feng J, et al. *Adv Mater* 2010;22:3723–8.
- [168] Fang Y, Luo B, Jia Y, Li X, Wang B, Song Q, et al. *Adv Mater* 2012;24:6348–55.
- [169] Rakhii RB, Chen W, Cha D, Alshareef HN. *Nano Lett* 2012;12:2559–67.
- [170] Chen Z, Augustyn V, Wen J, Zhang Y, Shen M, Dunn B, et al. *Adv Mater* 2011;23:791–5.
- [171] Chen W, Rakhii RB, Hu L, Xie X, Cui Y, Alshareef HN. *Nano Lett* 2011;11:5165–72.
- [172] Zhang F, Yuan C, Zhu J, Wang J, Zhang X, Lou XWD. *Adv Funct Mater* 2013;23:3909–15.
- [173] Yang S, Wu X, Chen C, Dong H, Hu W, Wang X. *Chem Commun* 2012;48:2773–5.
- [174] Chen Z, Yu D, Xiong W, Liu P, Liu Y, Dai L. *Langmuir* 2014;30:3567–71.
- [175] Hao L, Li X, Zhi L. *Adv Mater* 2013;25:3899–904.
- [176] Achilleos DS, Hatton TA. *J Colloid Interface Sci* 2015;447:282–301.
- [177] Brousse T, Bélanger D, Long JW. *J Electrochem Soc* 2015;162:A5185–9.
- [178] Kotal M, Thakur AK, Bhowmick AK. *ACS Appl Mater Interfaces* 2013;5:8374–86.
- [179] Zhao HB, Yang J, Lin TT, Lü QF, Chen G. *Chem A Eur J* 2015;21:682–90.
- [180] Haq AU, Lim J, Yun JM, Lee WJ, Han TH, Kim SO. *Small* 2013;9:3829–33.
- [181] Liu T, Finn L, Yu M, Wang H, Zhai T, Lu X, et al. *Nano Lett* 2014;14:2522–7.
- [182] Wang YG, Xia YY. *Electrochim Commun* 2005;7:1138–42.
- [183] Yu N, Gao L. *Electrochim Commun* 2009;11:220–2.
- [184] Yu G, Xie X, Pan L, Bao Z, Cui Y. *Nano Energy* 2013;2:213–34.
- [185] Hu CC, Chen JC, Chang KH. *J Power Sources* 2013;221:128–33.
- [186] Mosqueda HA, Crosnier O, Athouël L, Dandeville Y, Scudeller Y, Guillemet P, et al. *Electrochim Acta* 2010;55:7479–83.
- [187] Wang F, Xiao S, Hou Y, Hu C, Liu L, Wu Y. *RSC Adv* 2013;3:13059–84.
- [188] Qu Q, Zhang P, Wang B, Chen Y, Tian S, Wu Y, et al. *J Phys Chem C* 2009;113:14020–7.
- [189] Long JW, Bélanger D, Brousse T, Sugimoto W, Sassin MB, Crosnier O. *MRS Bull* 2011;36:513–22.
- [190] Guo D, Ren W, Chen Z, Mao M, Li Q, Wang T. *RSC Adv* 2015;5:10681–7.
- [191] Zhu M, Huang Y, Meng W, Gong Q, Li G, Zhi C. *J Mater Chem A* 2015;3:21321–7.
- [192] Chu HY, Lai QY, Hao YJ, Zhao Y, Xu XY. *J Appl Electrochem* 2009;39:2007–13.
- [193] Manivel A, Asiri AM, Alamry KA, Lana-Villarreal T, Anandan S. *Bull Mater Sci* 2014;4:861–9.
- [194] Yuksel R, Coskun S, Unalan HE. *Electrochim Acta* 2016;193:39–44.
- [195] Ghosh D, Giri S, Moniruzzaman M, Basu T, Mandal M, Das CK. *Dalton Trans* 2014;43:11067–76.
- [196] Khomenko V, Frackowiak E, Beguin F. *Electrochim Acta* 2005;50:2499–506.
- [197] Gryglewicz G, Machnikowski J, Lorenc-Grabowska E, Lota G, Frackowiak E. *Electrochim Acta* 2005;50:1197–206.
- [198] Kim J, Young C, Lee J, Park MS, Shahabuddin M, Yamauchi Y, et al. *Chem Commun* 2016;52:13016–9.
- [199] Guo L, Zhang L, Zhang J, Zhou J, He Q, Zeng S, et al. *Chem Commun* 2009;40:6071–3.
- [200] Shakir I, Shahid M, Cherevko S, Chung CH, Kang DJ. *Electrochim Acta* 2011;58:76–80.
- [201] Brousse T, Bélanger D, Guay D. Supercapacitors: materials, systems, and applications. Weinheim, Germany: Wiley-VCH Verlag GmbH & Co. KGaA; 2013. p. 257–88.
- [202] Algharaibeh ZA, Pickup PG. *Electrochim Soc* 2011;6. [170–170].
- [203] Ramkumar R, Sundaram MM. *New J Chem* 2016;40:2863–77.
- [204] Szweczyk A, Sikula J, Sedlakova V, Majzner J, Sedlak P, Kuparowitz T. *Met Meas Syst* 2016;23:403–11.
- [205] Shulga YM, Baskakov SA, Smirnov VA, Shulga NY, Belay KG, Gutsev GL. *J Power Sources* 2014;245:33–6.
- [206] Sennu P, Choi HJ, Baek SG, Aravindan V, Lee YS. *Carbon* 2016;98:58–66.
- [207] Jain A, Jayaraman S, Ulaganathan M, Balasubramanian R, Aravindan V, Srinivasan MP, et al. *Electrochim Acta* 2017;228:131–8.
- [208] Yuksel R, Coskun S, Kalay YE, Unalan HE. *Flexible. J Power Sources* 2016;328:167–73.
- [209] Aravindan V, Ulaganathan M, Madhavi S. *J Mater Chem A* 2016;4:7538–48.
- [210] Aricò AS, Bruce P, Scrosati B, Tarascon JM, Van Schalkwijk W. *Nat Mater* 2005;4:366–77.
- [211] Aleksenskii AE, Brunkov PN, Dideikin AT, Kirilenko DA, Kudashova YV, Sakseev DA, et al. *Tech Phys* 2013;58:1614–8.
- [212] Geim AK, Novoselov KS. *Nat Mater* 2007;6:183–91.
- [213] Tehrani Z, Thomas DJ, Korochkina T, Phillips CO, Lupo D, Lehtimäki S, et al. *Energy* 2017;118:1313–21.
- [214] Kim SG, Lee SS, Lee E, Yoon J, Lee HS. *RSC Adv* 2015;5:102567–73.
- [215] Zhan L, Huang D, Hu N, Yang C, Li M, Wei H, et al. *J Power Sources* 2017;342:1–8.
- [216] Yang C, Zhang L, Hu N, Yang Z, Su Y, Xu S, et al. *Chem Eng J* 2017;309:89–97.
- [217] Li B, Camilli CI, Xidas PI, Triantafyllidis KS, Manias E. *J Mat Res* 2017;32:12/28.
- [218] Szubda B, Szmaja A, Ozimek M, Mazurkiewicz S. *Appl Phys A* 2014;117:1801–9.
- [219] Lei Z, Christov N, Zhao XS. *Energy Environ Sci* 2011;4:1866–73.
- [220] Wu HC, Lin YP, Lee E, Lin WT, Hu JK, Chen HC, et al. *Mater Chem Phys* 2009;117:294–300.
- [221] Ye S, Kim LJ, Yang SH, Lee JW, Oh WC. *J Mater Sci Mater Electron* 2017;28:6592–600.
- [222] Obreja VV. *Nanostructures* 2008;40:2596–605.
- [223] Pan H, Li J, Feng Y. *Nanoscale Res Lett* 2010;5:654.
- [224] Kötter R, Carlen M. *Electrochim Acta* 2000;45:2483–98.
- [225] Arulepp M, Leis J, Lätt M, Miller F, Rumma K, Lust E, et al. *J Power Sources* 2006;2:1460–6.
- [226] Tang P, Zhao Y, Xu C, Ni K. *J Solid State Electrochem* 2013;17:1701–10.
- [227] Liu C, Yu Z, Neff D, Zhamu A, Jang BZ. *Nano Lett* 2010;10:4863–8.
- [228] Snook GA, Kao P, Best AS. *J Power Sources* 2011;196:1–12.
- [229] Lätt M, Käärrik M, Permann L, Kuura H, Arulepp M, Leis J. *J Solid State Electrochem* 2010;14:543–8.
- [230] Andreas HA, Conway BE. *Electrochim Acta* 2006;51:6510–20.
- [231] Yang Q, Lu Z, Sun X, Liu J. *Sci Rep* 2013;3:5371–7.
- [232] Padmanathan N, Selladurai S, Razeed KM. *RSC Adv* 2015;5:12700–9.
- [233] Vlad A, Singh N, Rolland J, Melinte S, Ajayan PM, Gohy JF. *Sci Rep* 2014;4:4315.
- [234] Gogotsi Y, Simon P. *Science* 2011;334:917–8.
- [235] Sun W, Zheng R, Chen X. *J Power Sources* 2010;195:7120–5.
- [236] Bruce PG, Freunberger SA, Hardwick LJ, Tarascon JM. *Nat Mater* 2012;11:19–29.
- [237] Kobayashi M, Colaneri N, Boysel M, Wudl F, Heeger AJ. *J Chem Phys* 1985;82:5717–23.
- [238] Galiński M, Lewandowski A, Stepniak I. *Electrochim Acta* 2006;51:5567–80.
- [239] Han H, Cho S. *Nanomaterials* 2018;8:726.
- [240] Akbulut S, Yilmaz M, Raina S, Hsu SH, Kang WP. *J Appl Electrochem* 2017;47:1035–44.
- [241] <<http://gronnfase.blogspot.com/2014/10/supercapacitors-for-peak-shifting-over.html>>.
- [242] Zheng G, Hu L, Wu H, Xie X, Cui Y. *Energy Environ Sci* 2011;4:3368–73.
- [243] Huang S, Wen Z, Zhu X, Gu Z. *Electrochim Commun* 2004;6:1093–7.
- [244] Naoi K, Ishimoto S, Isobe Y, Aoyagi S. *J Power Sources* 2010;195:6250–4.
- [245] Naoi K, Ishimoto S, Ogihara N, Nakagawa Y, Hatta S. *J Electrochem Soc* 2009;156:A52–9.
- [246] Cameron CG. *ECS Trans* 2012;41:121–32.
- [247] Cresce A, Borodin O, Xu K. *J Phys Chem C* 2012;116:26111–7.
- [248] Dennison CR, Beidaghi M, Hatzell KB, Campos JW, Gogotsi Y, Kumbur EC. *J Power Sources* 2014;24:489–96.
- [249] Münchgesang W, Meisner P, Yushin G. *AIP Conf Proc* 2014;1597:196–203.
- [250] Tey JP, Careem MA, Yarmo MA, Arof AK. *Ionics* 2016;22:1209–16.

- [251] Schneuwly A, Gallay R. In: Proceedings of the power conversion and intelligent motion conference. Nurnberg, Germany: PCIM; 2000.
- [252] Park DW, Cañas NA, Schwan M, Milow B, Ratke L, Friedrich KA. *Curr Appl Phys* 2016;16:658–64.
- [253] Bian W, Zhu S, Qi M, Xiao L, Liu Z, Zhan J. *Anal Methods* 2017;9:459–64.
- [254] <[http://www.aowei.com/case\\_view.php?typeid=1&id=4](http://www.aowei.com/case_view.php?typeid=1&id=4)>.
- [255] Miller JR, Burke AF. *Electrochem Soc Int* 2008;17:53–7.
- [256] 4 Neo Green Power (<[http://www.adetelgroup.com/library/fichesproduits/4NEO\\_GREEN\\_POWER.pdf](http://www.adetelgroup.com/library/fichesproduits/4NEO_GREEN_POWER.pdf)>).
- [257] Supercapacitor energy storage for South Island Line. *Railway Gazette*. 20120803. Retrieved 2013-05-29.
- [258] Cantec Systems, Power solutions (<<http://www.cantecsystems.com/>>). 132.
- [259] Evans Capacitor Company. High Energy Density Capacitors for Military Applications (<[http://www.evanscap.com/pdf/Hybrid\\_Caps\\_COTS.pdf](http://www.evanscap.com/pdf/Hybrid_Caps_COTS.pdf)>).
- [260] Walkowiak M, Wasinski K, Polrolniczak P, Martyla A, Waszak D, Surendran AA, et al. *ECS Trans* 2015;70:27–36.
- [261] Tecate group. Backup power for military applications batteries optional! (<<http://www.tecategroup.com/ultracapacitorssupercapacitors/militaryapplications.php>>).
- [262] Endo M, Maeda T, Takeda T, Kim YJ, Koshiba K, Hara H, et al. *J Electrochem Soc* 2001;148:A910–4.
- [263] Chen K, Xue D. Colloidal supercapacitor electrode materials. *Mater Res Bull* 2016;83:201–6.
- [264] Drew J. Supercapacitor-based power backup system protects volatile data in handhelds when power is lost, in design note 498; 2011. Available from: <<http://www.linear.com/>>.
- [265] yec.com.tw. Super capacitor supplier list | YEC | This high energy capacitor from a defibrillator can deliver a lethal 500 J of energy. YEC. Retrieved 20130529.
- [266] Kumar SN, Renuga P, Svc VC. *Int J Power Energy Syst* 2012;32:49–56.
- [267] FastCap. Introducing FastCAP's ulysses power systems for drilling applications. 2013<<http://www.fastcapsystems.com/products>>.
- [268] <<http://toolmonger.com/2007/11/05/ultracapacitors-the-next-source-for-powerful-cordless-tools/>>.
- [269] Wang X, Yang C, Wang G. *J Mater Chem A* 2016;4:14839–48.
- [270] Kazaryan S. In: Proceedings of advanced capacitor world summit. Hilton San Diego Resort, San Diego, CA; 2007.
- [271] Aravindan V, Cheah YL, Mak WF, Wee G, Chowdari BV, Madhavi S. *Chem Plus Chem* 2012;77:570–5.
- [272] Park GJ, Kalpana D, Thapa AK, Nakamura H, Lee YS, Yoshio M. *Bull Korean Chem Soc* 2009;30:817–20.
- [273] Fan Z, Yan J, Zhi L, Zhang Q, Wei T, Feng J, et al. *Adv Mater* 2010;22:3723–8.
- [274] Fang Y, Luo B, Jia Y, Li X, Wang B, Song Q, et al. *Adv Mater* 2012;24:6348–55.
- [275] Cole DP, Reddy ALM, Hahm MG, McCotter R, Hart AH, Vajtai R, et al. *Adv Energy Mater* 2014;4:1300844.